

Benign Landscape of Quadratic Programs with Orthogonality Constraints and Its Application to Heteroscedastic Probabilistic PCA*

Peng Wang[†] Po Chen[‡] Rujun Jiang[§] Laura Balzano[¶]

June 26, 2026

Abstract

In this work, we study the optimization landscape of homogeneous quadratic programs with orthogonality constraints (QPOC) and apply the resulting theory to heteroscedastic probabilistic PCA (HePPCA). For QPOC, we establish a complete characterization of the benign optimization landscape by showing that every critical point is either a global maximizer or a strict saddle point. Our analysis builds on a closed-form characterization of the critical point set, from which we derive a necessary and sufficient condition for global optimality and show that every non-optimal critical point has a direction of positive curvature. As an application, we show that the population version of HePPCA is a special instance of QPOC and therefore has a benign optimization landscape; moreover, it satisfies local geodesic strong concavity near every global maximizer. We furthermore prove that, when the sample size is sufficiently large, the sample version of HePPCA inherits these favorable properties with high probability. Together with existing theory on avoiding strict saddle points, our results provide a theoretical justification for the observed local linear convergence of retraction-based optimization methods to global solutions for both QPOC and HePPCA. Finally, we present numerical experiments to corroborate our theoretical results.

1 Introduction

In this work, we study the following homogeneous quadratic program with orthogonality constraints (QPOC):

$$\max_{\mathbf{Q} \in \mathbb{R}^{d \times K}} F(\mathbf{Q}) := \text{Tr}(\mathbf{Q}^T \mathbf{A} \mathbf{Q} \mathbf{B}) \quad \text{s.t. } \mathbf{Q} \in \text{St}(d, K). \quad (1)$$

Here, $\text{St}(d, K) = \{\mathbf{Q} \in \mathbb{R}^{d \times K} : \mathbf{Q}^T \mathbf{Q} = \mathbf{I}_K\}$ denotes the Stiefel manifold with $d \geq K$, \mathbf{I}_K is the $K \times K$ identity matrix, and $\mathbf{A} \in \mathbb{R}^{d \times d}$ and $\mathbf{B} \in \mathbb{R}^{K \times K}$ are symmetric matrices. This is a

*The first and second authors equally contribute to this work.

[†]Department of Computer and Information Science, University of Macau, Macao SAR, China (pengw@um.edu.mo).

[‡]School of Data Science, Fudan University, Shanghai, China (chenp24@m.fudan.edu.cn).

[§]School of Data Science, Fudan University, Shanghai, China (rjjiang@fudan.edu.cn).

[¶]Department of Electrical Engineering and Computer Science, University of Michigan, Ann Arbor, USA (girasole@umich.edu).

classical and important class of matrix optimization problems, which has been widely studied in applied mathematics, machine learning, and signal processing. It includes several well-known formulations as special cases, such as eigenvalue problems [12], generalized eigenvalue problems [14], and orthogonal relaxations of quadratic assignment problems [15].

Over the past few decades, Problem (1) has been extensively studied, with particular focus on algorithm design and the analysis of its optimization properties. A variety of algorithms have been proposed for solving this problem by exploiting its structure, including Riemannian gradient descent [3, 23], projected gradient descent [27], and exact penalty function methods [28, 29], to name a few. These methods leverage the geometry of the Stiefel manifold or incorporate penalty terms to enforce the constraints, providing both theoretical convergence guarantees and strong empirical performance. An influential work [20] demonstrated that the Lojasiewicz exponent at any critical point of Problem (1) is $1/2$. This result implies that a broad class of first-order retraction-based methods for solving this problem enjoys local linear convergence to a critical point. Interestingly, empirical observations demonstrate that these methods often converge to a global maximizer of Problem (1), rather than merely a generic critical point (see Figure 2). This naturally raises the question of whether the optimization landscape of Problem (1) is benign, in the sense that each critical point is either a global maximizer or a strict saddle point (see Definition 1).

Our first contribution is to provide an affirmative answer to the above question by showing that Problem (1) indeed has a benign optimization landscape. To this end, we first review the closed-form characterization of the critical point set in [20]. Building on this characterization, we identify a sufficient condition for global optimality (see Proposition 1). We then show that any critical point violating this condition is a strict saddle point by constructing a direction of positive curvature (see Proposition 2). Consequently, this condition is also necessary. These results yield a complete characterization of the optimization landscape (see Theorem 2). Combined with strict-saddle avoidance [16] and the Lojasiewicz exponent in [20], this explains why retraction-based methods usually converge to a global maximizer at a locally linear rate.

Our second contribution is the application of the above results to the HePPCA problem [9, 13, 25]. The HePPCA model extends the classical PCA model by allowing samples from different groups to have different noise variances, enabling more accurate modeling of data with heterogeneous variability across groups (see (24)). We study the maximum likelihood estimation problem of the HePPCA model, as formulated in Problem (25). Under the HePPCA model assumptions, we show that the population version of Problem (25) is a special instance of Problem (1) and therefore admits a benign optimization landscape. Moreover, we prove that it is locally geodesically strongly concave on the Stiefel manifold near every global maximizer. Building on this, we conduct a perturbation analysis and show that, when the sample size is sufficiently large, Problem (25) admits the same properties as its population counterpart with high probability (see Theorem 4). This result is significant, as it shows that retraction-based optimization methods converge to global solutions of the HePPCA problem at a locally linear rate.

1.1 Related Work

In non-convex optimization, a common approach to understanding the behavior of optimization algorithms is through the analysis of the optimization landscape [1, 6, 7, 17, 24, 26]. By characterizing the landscape, one can identify different types of critical points, including local minimizers, global minimizers, strict saddle points, and non-strict saddle points (see Definition 1). In particular, a non-convex problem is said to admit a *benign optimization landscape* if every critical point is either a strict saddle point or a global minimizer.¹ Typical examples of such problems include neural collapse problems [32, 34], low-rank matrix recovery [2, 8], and group synchronization [22, 21]. Moreover, the foundational work [16] showed that first-order methods, including gradient descent, manifold gradient descent, block coordinate descent, and their variants, avoid strict saddle points for almost all initializations. Consequently, for a problem with a benign landscape, randomly initialized first-order methods almost always converge to globally optimal points.

We next review recent advances in the analysis of optimization landscapes for smooth problems over manifolds. McRae and Boumal [21] studied the Burer-Monteiro relaxation of the orthogonal group synchronization problem, which maximizes a quadratic problem over the Stiefel manifold. They proved that it has a benign optimization landscape when the relaxation rank is larger than a threshold. Ling [18, 19] studied the same relaxation problem and showed that it possesses a unique local minimizer, which is also global under mild conditions. Recently, McRae et al. [22] derived a sufficient condition under which the Burer-Monteiro relaxation of the Z_2 synchronization problem, which lies on the oblique manifold, has a benign optimization landscape under mild conditions on the measurement graph and noise. Yaras et al. [32] studied the cross-entropy loss for optimizing two-layer linear networks over the oblique manifold and showed that this problem has a benign optimization landscape.

Now we turn to literature on the heteroscedastic PCA problem. HePPCA extends classical PCA by incorporating heterogeneous probabilistic priors into the dimensionality reduction framework. Hong et al. [13] developed a HePPCA model that accounts for heteroscedastic noise across samples and derived the corresponding maximum likelihood estimation formulation. Based on this, they proposed efficient alternating maximization algorithms to jointly estimate both underlying factors and noise variances. Gilman et al. [9] considered the setting where the noise variances for each data group are known and formulated HePPCA as a sum of heterogeneous quadratic functions on the Stiefel manifold. They studied a semidefinite relaxation of this problem and established a certificate for global optimality. Recently, Wang et al. [25] proposed a generalized power method for solving the same formulation and provided estimation guarantees based on an error-bound property.

Beyond the aforementioned line of research, many other works have also explored different aspects and formulations of HePPCA. Zhang et al. [33] proposed a HeteroPCA algorithm for principal component analysis under heteroscedastic noise across features (as opposed to heteroscedasticity across samples) and proved its optimality under a generalized spiked covariance model via robust subspace perturbation analysis. Building on this work, Yan et al. [31]

¹This definition is stated for minimization problems. In our setting, we consider a maximization problem, and the definition is adapted accordingly.

developed non-asymptotic distributional guarantees for HeteroPCA and demonstrated that it enables accurate inference for the principal subspace, even in the presence of missing data. For heteroscedasticity across samples, further extensions and algorithmic developments include the ALPCAH method, which addresses sample-wise heteroscedastic PCA with robust subspace estimation [4]; streaming HePPCA, which is designed for online or sequential data with heteroscedastic noise [10]; and the HeMPPCAT mixture model, which generalizes HePPCA to mixtures of probabilistic PCA components with heterogeneous noise across components [30].

1.2 Notation and Organization

We use \mathbb{S}^n to denote the set of all $n \times n$ symmetric matrices. For a positive integer n , let $[n] := \{1, \dots, n\}$. For a finite set \mathcal{S} , we use $|\mathcal{S}|$ to denote its cardinality. Given scalars a_1, \dots, a_n , we define $a_{\max} := \max\{a_i : i \in [n]\}$ and $a_{\min} := \min\{a_i : i \in [n]\}$. Given a vector \mathbf{a} , let $\|\mathbf{a}\|$ denote its Euclidean norm, a_i its i -th entry, and $\text{diag}(\mathbf{a})$ the diagonal matrix with \mathbf{a} on its diagonal. For a matrix \mathbf{A} , we define $\|\mathbf{A}\|$ as its spectral norm, $\|\mathbf{A}\|_F$ as its Frobenius norm, a_{ij} or $\mathbf{A}(i, j)$ as its (i, j) -th entry, and $\sigma_i(\mathbf{A})$ as its i -th largest singular value. For an integer n , let \mathcal{P}^n denote the set of all $n \times n$ permutation matrices. We associate each $\mathbf{\Pi} \in \mathcal{P}^n$ with a permutation $\pi : [n] \rightarrow [n]$ through the convention that $\mathbf{\Pi}(i, j) = 1$ if $j = \pi(i)$ and $\mathbf{\Pi}(i, j) = 0$ otherwise for all $i, j \in [n]$. Under this convention, $\mathbf{\Pi}\mathbf{e}_i = \mathbf{e}_{\pi^{-1}(i)}$, $\mathbf{\Pi}^T\mathbf{e}_i = \mathbf{e}_{\pi(i)}$, and, for any diagonal matrix \mathbf{D} , $(\mathbf{\Pi}^T\mathbf{D}\mathbf{\Pi})(i, i) = \mathbf{D}(\pi^{-1}(i), \pi^{-1}(i))$. We use \mathcal{O}^n to denote the set of $n \times n$ orthogonal matrices. The symbol $\mathbf{a} \circ \mathbf{b}$ denotes the Hadamard product of two vectors $\mathbf{a}, \mathbf{b} \in \mathbb{R}^n$, i.e., $\mathbf{a} \circ \mathbf{b} = (a_1b_1, \dots, a_nb_n)$. We denote by $\text{BlkD}(\mathbf{X}_1, \dots, \mathbf{X}_n)$ the block diagonal matrix with diagonal blocks $\mathbf{X}_1, \dots, \mathbf{X}_n$. Blocks with zero rows or zero columns are allowed and are simply omitted from displayed block matrices. In particular, $\mathbf{X}_i \in \mathbb{R}^{m_i \times 0}$ contributes only m_i rows and $\mathbf{X}_i \in \mathbb{R}^{0 \times n_i}$ contributes only n_i columns.

Given $\mathbf{Q} \in \text{St}(d, K)$, the tangent space to $\text{St}(d, K)$ at \mathbf{Q} is

$$\text{T}(\mathbf{Q}) = \left\{ \mathbf{X} \in \mathbb{R}^{d \times K} : \text{sym}(\mathbf{Q}^T \mathbf{X}) = \mathbf{0} \right\},$$

where $\text{sym}(\mathbf{C}) := (\mathbf{C} + \mathbf{C}^T)/2$. According to [3, page 162], the projection onto the tangent space of $\text{St}(d, K)$ is $\text{Proj}_{\text{T}(\mathbf{Q})}(\mathbf{C}) = \mathbf{C} - \mathbf{Q}\text{sym}(\mathbf{Q}^T \mathbf{C})$. Given a smooth function $F : \mathbb{R}^{d \times K} \rightarrow \mathbb{R}$, its Riemannian gradient on the Stiefel manifold at \mathbf{Q} can be calculated as

$$\text{grad } F(\mathbf{Q}) = \text{Proj}_{\text{T}(\mathbf{Q})}(\nabla F(\mathbf{Q})).$$

The Riemannian Hessian at \mathbf{Q} along the direction $\mathbf{D} \in \text{T}(\mathbf{Q})$ can be calculated as

$$\text{Hess } F(\mathbf{Q})[\mathbf{D}] = \text{Proj}_{\text{T}(\mathbf{Q})}(\nabla^2 F(\mathbf{Q})[\mathbf{D}] - \mathbf{D}\text{sym}(\mathbf{Q}^T \nabla F(\mathbf{Q}))) \quad (2)$$

We also write $\text{Hess } F(\mathbf{Q})[\mathbf{D}, \mathbf{D}] := \langle \mathbf{D}, \text{Hess } F(\mathbf{Q})[\mathbf{D}] \rangle$.

Now, we formally introduce the definitions of global maximizers, local maximizers, critical points, and strict saddle points for the problem of maximizing a smooth function $H(\mathbf{Q})$ over the Stiefel manifold:

$$\max_{\mathbf{Q} \in \mathbb{R}^{d \times K}} H(\mathbf{Q}) \quad \text{s.t. } \mathbf{Q} \in \text{St}(d, K). \quad (3)$$

Definition 1. For Problem (3), we say that

- (i) $\mathbf{Q}^* \in \text{St}(d, K)$ is a global maximizer if $H(\mathbf{Q}^*) \geq H(\mathbf{Q})$ for all $\mathbf{Q} \in \text{St}(d, K)$.
- (ii) \mathbf{Q}^* is a local maximizer if there exists a neighborhood \mathcal{U} of \mathbf{Q}^* such that $H(\mathbf{Q}^*) \geq H(\mathbf{Q})$ for all $\mathbf{Q} \in \mathcal{U} \cap \text{St}(d, K)$.
- (iii) $\mathbf{Q}^* \in \text{St}(d, K)$ is a critical point if $\text{grad } H(\mathbf{Q}^*) = \mathbf{0}$.
- (iv) $\mathbf{Q}^* \in \text{St}(d, K)$ is a strict saddle point² if it is a critical point and $\text{Hess } H(\mathbf{Q}^*)[\mathbf{D}, \mathbf{D}] > 0$ for a nonzero direction $\mathbf{D} \in \text{T}(\mathbf{Q}^*)$.

The rest of this paper is organized as follows. In Section 2, we review existing closed-form characterizations of the critical point set of Problem (1). In Section 3, we present the optimization landscape result for Problem (1). In Section 4, we extend these results to study the optimization landscape of the HePPCA problem. Finally, Section 5 presents numerical experiments, and Section 6 concludes the paper.

2 Preliminaries

In this section, we present the problem setup and review a key result from [20] that gives a closed-form characterization of the critical point set of Problem (1) when \mathbf{B} is nonsingular. We then extend it to the singular case.

To proceed, let $\mathbf{A} = \mathbf{U}_A \mathbf{\Lambda}_A \mathbf{U}_A^T$ and $\mathbf{B} = \mathbf{U}_B \mathbf{\Lambda}_B \mathbf{U}_B^T$ be spectral decompositions of $\mathbf{A} \in \mathbb{S}^d$ and $\mathbf{B} \in \mathbb{S}^K$, respectively, where $\mathbf{U}_A \in \mathcal{O}^d$ and $\mathbf{U}_B \in \mathcal{O}^K$. It is straightforward to verify that $\text{Tr}(\mathbf{Q}^T \mathbf{A} \mathbf{Q} \mathbf{B}) = \text{Tr}(\bar{\mathbf{Q}}^T \mathbf{\Lambda}_A \bar{\mathbf{Q}} \mathbf{\Lambda}_B)$, where $\bar{\mathbf{Q}} = \mathbf{U}_A^T \mathbf{Q} \mathbf{U}_B \in \text{St}(d, K)$. The map $\mathbf{Q} \mapsto \mathbf{U}_A^T \mathbf{Q} \mathbf{U}_B$ is a bijective isometry of the Stiefel manifold under the embedded Euclidean metric. Therefore, we assume without loss of generality that

$$\mathbf{A} = \text{diag}(a_1, \dots, a_d), \quad \mathbf{B} = \text{diag}(b_1, \dots, b_K), \quad (4)$$

where $a_1 \geq a_2 \geq \dots \geq a_d$ and $b_1 \geq b_2 \geq \dots \geq b_K$. For ease of exposition, we denote the critical point set of Problem (1) by $\mathcal{Q} := \{\mathbf{Q} \in \text{St}(d, K) : \text{grad} F(\mathbf{Q}) = \mathbf{0}\}$. By [20, Proposition 1], this set can be written as

$$\mathcal{Q} = \{\mathbf{Q} \in \text{St}(d, K) : \mathbf{A} \mathbf{Q} \mathbf{B} - \mathbf{Q} \mathbf{B} \mathbf{Q}^T \mathbf{A} \mathbf{Q} = \mathbf{0}\}. \quad (5)$$

Nonsingular \mathbf{B} We first consider the case where \mathbf{B} is nonsingular, i.e., $b_i \neq 0$ for each $i \in [K]$. In this case, Liu et al. [20] derived a closed-form expression for \mathcal{Q} . Specifically, let n_A and n_B be the numbers of distinct eigenvalues of \mathbf{A} and \mathbf{B} , respectively. We assume that $n_A \geq 2$, as the objective function is a constant when $n_A = 1$ and all feasible points are trivially optimal. Then, there exist indices s_0, s_1, \dots, s_{n_A} and t_0, t_1, \dots, t_{n_B} that partition the eigenvalues into groups of equal value, such that $0 = s_0 < s_1 < \dots < s_{n_A} = d$, $0 = t_0 < t_1 < \dots < t_{n_B} = K$, and

$$\begin{aligned} a_{s_0+1} &= \dots = a_{s_1} > a_{s_1+1} = \dots = a_{s_2} > \dots > a_{s_{n_A-1}+1} = \dots = a_{s_{n_A}}, \\ b_{t_0+1} &= \dots = b_{t_1} > b_{t_1+1} = \dots = b_{t_2} > \dots > b_{t_{n_B-1}+1} = \dots = b_{t_{n_B}}. \end{aligned}$$

²For maximization problems, a direction of positive curvature is an escaping direction [16]. Note that this definition of strict saddle points therefore includes minima.

This, together with (4), allows us to express $\mathbf{A} \in \mathbb{S}^d$ and $\mathbf{B} \in \mathbb{S}^K$ as

$$\mathbf{A} = \text{BlkD} \left(a_{s_1} \mathbf{I}_{s_1-s_0}, \dots, a_{s_{n_A}} \mathbf{I}_{s_{n_A}-s_{n_A-1}} \right) \in \mathbb{S}^d, \quad (6)$$

$$\mathbf{B} = \text{BlkD} \left(b_{t_1} \mathbf{I}_{t_1-t_0}, \dots, b_{t_{n_B}} \mathbf{I}_{t_{n_B}-t_{n_B-1}} \right) \in \mathbb{S}^K, \quad (7)$$

respectively. We work with this form as opposed to (4) in order to handle rotational invariance that arises when eigenvalues have multiplicity greater than 1. Define

$$\mathcal{H} := \left\{ (h_1, \dots, h_{n_A}) : \sum_{i=1}^{n_A} h_i = K, h_i \in \{0, 1, \dots, s_i - s_{i-1}\}, i \in [n_A] \right\}.$$

In addition, given any $\mathbf{h} = (h_1, \dots, h_{n_A}) \in \mathcal{H}$, define

$$\begin{aligned} \mathbf{E}_i(\mathbf{h}) &:= [\mathbf{e}_{s_{i-1}+1} \cdots \mathbf{e}_{s_{i-1}+h_i}] \in \mathbb{R}^{d \times h_i} \quad \text{for } i = 1, \dots, n_A, \\ \mathbf{E}(\mathbf{h}) &:= [\mathbf{E}_1(\mathbf{h}), \dots, \mathbf{E}_{n_A}(\mathbf{h})] \in \mathbb{R}^{d \times K}, \end{aligned}$$

where $\{\mathbf{e}_i\}_{i=1}^d$ is the standard basis of \mathbb{R}^d .³ Intuitively, \mathbf{h} records how many basis vectors are selected from each eigenspace of \mathbf{A} . The matrix $\mathbf{E}(\mathbf{h})$ acts as a selector: for any compatible matrix \mathbf{W} , the product $\mathbf{W}\mathbf{E}(\mathbf{h})$ keeps the columns of \mathbf{W} indexed by these selected basis vectors. According to [20], the critical point set of Problem (1) admits the following closed-form expression.

Fact 1. ([20, Proposition 3]) *Suppose that $\mathbf{A} \in \mathbb{S}^d$ and $\mathbf{B} \in \mathbb{S}^K$ are given by (6) and (7), respectively, and that $b_i \neq 0$ for each $i \in [K]$. Then the critical point set \mathcal{Q} can be expressed as*

$$\mathcal{Q} = \bigcup_{\mathbf{h} \in \mathcal{H}, \mathbf{\Pi} \in \mathcal{P}^K} \mathcal{Q}_{\mathbf{h}, \mathbf{\Pi}},$$

where every $\mathcal{Q} \in \mathcal{Q}_{\mathbf{h}, \mathbf{\Pi}}$ can be written as

$$\mathcal{Q} = \text{BlkD}(\mathbf{U}_1, \dots, \mathbf{U}_{n_A}) \mathbf{E}(\mathbf{h}) \mathbf{\Pi} \text{BlkD}(\mathbf{V}_1^T, \dots, \mathbf{V}_{n_B}^T)$$

for some $\mathbf{U}_i \in \mathcal{O}^{s_i - s_{i-1}}$ for each $i \in [n_A]$ and $\mathbf{V}_j \in \mathcal{O}^{t_j - t_{j-1}}$ for each $j \in [n_B]$.

Singular \mathbf{B} We now extend the above result to the case where \mathbf{B} is singular but nonzero, and derive a closed-form expression for \mathcal{Q} . With a slight abuse of notation, let n_B denote the number of distinct nonzero eigenvalues of \mathbf{B} . After reordering the diagonal blocks, we write the zero block last and set $t_{n_B} = \text{rank}(\mathbf{B})$. Similar to the nonsingular case, there exist indices $t_0, t_1, \dots, t_{n_B}, t_{n_B+1}$ and $p \in \{0, 1, \dots, n_B\}$ such that $0 = t_0 < t_1 < \dots < t_{n_B} < t_{n_B+1} = K$ and

$$\begin{aligned} b_{t_{0+1}} &= \dots = b_{t_1} > \dots > b_{t_{p-1}+1} = \dots = b_{t_p} > 0, \\ 0 > b_{t_{p+1}} &= \dots = b_{t_{p+1}} > \dots > b_{t_{n_B-1}+1} = \dots = b_{t_{n_B}}, \\ b_{t_{n_B+1}} &= \dots = b_{t_{n_B+1}} = 0. \end{aligned}$$

³By convention, $h_i = 0$ means that $\mathbf{E}_i(\mathbf{h})$ is not included in $\mathbf{E}(\mathbf{h})$ for each $i \in [n_A]$.

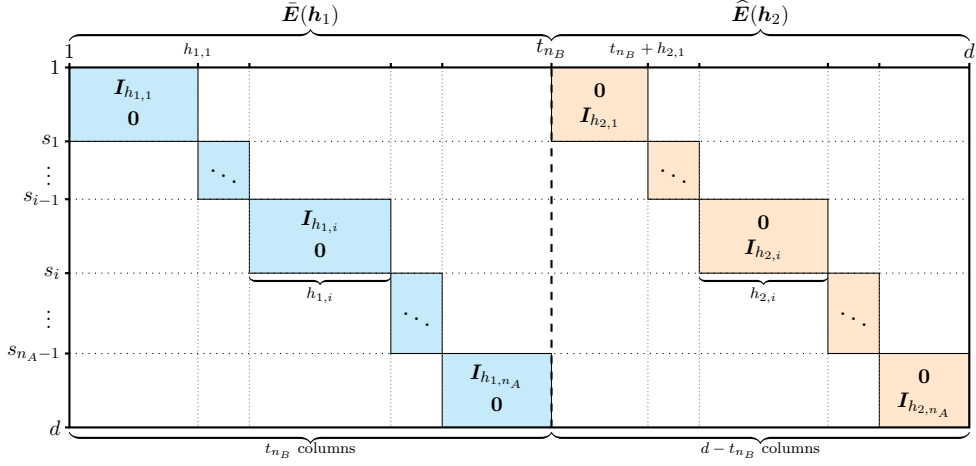


Figure 1: Visualization of the block structure of matrix $\mathbf{E}(\mathbf{h})$ defined in (11). All entries in the unshaded regions are zero.

In particular, $p = 0$ (resp., $p = n_B$) indicates that there does not exist an index i satisfying $b_i > 0$ (resp., $b_i < 0$). This partition differs from the decreasing-order partition only in that all zero entries are placed in the last block; either sign part may be empty. Therefore, we have

$$\mathbf{B} = \text{BlkD}(\widehat{\mathbf{B}}, \mathbf{0}_{K-t_{n_B}}), \quad \widehat{\mathbf{B}} = \text{BlkD}\left(b_{t_1} \mathbf{I}_{t_1-t_0}, \dots, b_{t_{n_B}} \mathbf{I}_{t_{n_B}-t_{n_B-1}}\right). \quad (8)$$

Substituting this form into (5), together with the argument in [20, Section 3.1.4], yields that the critical point set \mathcal{Q} of Problem (1) is equivalent to

$$\begin{aligned} \mathcal{Q} &= \{\mathbf{Q} = [\mathbf{Q}_1, \mathbf{Q}_2] \in \text{St}(d, K) : \mathbf{Q}_1 \in \mathcal{Q}_1\}, \\ \mathcal{Q}_1 &:= \left\{ \mathbf{Y} \in \text{St}(d, t_{n_B}) : \mathbf{A}\mathbf{Y}\widehat{\mathbf{B}} - \mathbf{Y}\widehat{\mathbf{B}}\mathbf{Y}^T\mathbf{A}\mathbf{Y} = \mathbf{0} \right\}. \end{aligned} \quad (9)$$

Now, we derive an explicit expression for \mathcal{Q} based on Fact 1. Define

$$\widetilde{\mathcal{H}} := \left\{ (\mathbf{h}_1, \mathbf{h}_2) : \begin{aligned} &\mathbf{h}_1 = (h_{1,1}, h_{1,2}, \dots, h_{1,n_A}), \quad \mathbf{h}_2 = (h_{2,1}, h_{2,2}, \dots, h_{2,n_A}), \\ &h_{1,i} \in \{0, 1, \dots, s_i - s_{i-1}\}, \quad i \in [n_A], \quad \sum_{i=1}^{n_A} h_{1,i} = t_{n_B}, \\ &h_{2,i} = s_i - s_{i-1} - h_{1,i}, \quad i \in [n_A] \end{aligned} \right\}.$$

In addition, given any $\mathbf{h} = (\mathbf{h}_1, \mathbf{h}_2) \in \widetilde{\mathcal{H}}$, define

$$\begin{aligned} \bar{\mathbf{E}}_i(\mathbf{h}_1) &:= [\mathbf{e}_{s_{i-1}+1} \cdots \mathbf{e}_{s_{i-1}+h_{1,i}}] \in \mathbb{R}^{d \times h_{1,i}} \text{ for each } i \in [n_A] \\ \widehat{\mathbf{E}}_i(\mathbf{h}_2) &:= [\mathbf{e}_{s_{i-1}+h_{1,i}+1} \cdots \mathbf{e}_{s_i}] \in \mathbb{R}^{d \times h_{2,i}} \text{ for each } i \in [n_A], \\ \bar{\mathbf{E}}(\mathbf{h}_1) &:= [\bar{\mathbf{E}}_1(\mathbf{h}_1) \cdots \bar{\mathbf{E}}_{n_A}(\mathbf{h}_1)] \in \mathbb{R}^{d \times t_{n_B}}, \end{aligned} \quad (10)$$

$$\begin{aligned} \widehat{\mathbf{E}}(\mathbf{h}_2) &:= [\widehat{\mathbf{E}}_1(\mathbf{h}_2) \cdots \widehat{\mathbf{E}}_{n_A}(\mathbf{h}_2)] \in \mathbb{R}^{d \times (d-t_{n_B})}, \\ \mathbf{E}(\mathbf{h}) &:= [\bar{\mathbf{E}}(\mathbf{h}_1) \widehat{\mathbf{E}}(\mathbf{h}_2)] \in \mathbb{R}^{d \times d}. \end{aligned} \quad (11)$$

To illustrate this construction, we provide a schematic illustration of the matrix $\mathbf{E}(\mathbf{h})$ in Figure 1.

Theorem 1. Suppose that $\mathbf{A} \in \mathbb{S}^d$ is in the form (6) and $\mathbf{B} \in \mathbb{S}^K$ is singular but nonzero, and is in the form (8). Then the set \mathcal{Q} can be expressed as

$$\mathcal{Q} = \bigcup_{\mathbf{h} \in \tilde{\mathcal{H}}, \mathbf{\Pi} \in \mathcal{P}^{t_{n_B}}} \mathcal{Q}_{\mathbf{h}, \mathbf{\Pi}},$$

where every $\mathbf{Q} \in \mathcal{Q}_{\mathbf{h}, \mathbf{\Pi}}$ takes the form

$$\mathbf{Q} = \text{BlkD}(\mathbf{U}_1, \dots, \mathbf{U}_{n_A}) \left[\bar{\mathbf{E}}(\mathbf{h}_1) \mathbf{\Pi} \hat{\mathbf{E}}(\mathbf{h}_2) \mathbf{V}_{n_B+1} \right] \text{BlkD}(\mathbf{V}_1^T, \dots, \mathbf{V}_{n_B}^T, \mathbf{I}_{K-t_{n_B}}) \quad (12)$$

for some $\mathbf{U}_i \in \mathcal{O}^{s_i-s_{i-1}}$ for each $i \in [n_A]$, $\mathbf{V}_j \in \mathcal{O}^{t_j-t_{j-1}}$ for each $j \in [n_B]$, and $\mathbf{V}_{n_B+1} \in \text{St}(d-t_{n_B}, K-t_{n_B})$.

Proof. Using $\bar{\mathbf{E}}_i(\mathbf{h}_1)^T \hat{\mathbf{E}}_i(\mathbf{h}_2) = \mathbf{0}$ for each $i \in [n_A]$, it is straightforward to verify that every $\mathbf{Q} \in \mathcal{Q}_{\mathbf{h}, \mathbf{\Pi}}$ of the form (12) satisfies $\mathbf{A}\mathbf{Q}\mathbf{B} - \mathbf{Q}\mathbf{B}\mathbf{Q}^T\mathbf{A}\mathbf{Q} = \mathbf{0}$, and thus $\text{grad}F(\mathbf{Q}) = \mathbf{0}$.

Using the equivalence between (5) and (9), it suffices to take an arbitrary $\mathbf{Q} = [\mathbf{Q}_1, \mathbf{Q}_2] \in \mathcal{Q}$ as in (9) and show that it admits the representation (12). We note that \mathcal{Q}_1 in (9) coincides with the critical point set of the following QPOC problem

$$\max_{\mathbf{Q} \in \text{St}(d, t_{n_B})} \text{Tr}(\mathbf{Q}^T \mathbf{A} \mathbf{Q} \hat{\mathbf{B}}).$$

By Fact 1, every $\mathbf{Q}_1 \in \mathcal{Q}_1$ admits the representation

$$\mathbf{Q}_1 = \text{BlkD}(\mathbf{U}_1, \dots, \mathbf{U}_{n_A}) \bar{\mathbf{E}}(\mathbf{h}_1) \mathbf{\Pi} \text{BlkD}(\mathbf{V}_1^T, \dots, \mathbf{V}_{n_B}^T),$$

where $\mathbf{U}_i \in \mathcal{O}^{s_i-s_{i-1}}$ for all $i \in [n_A]$, $\mathbf{V}_j \in \mathcal{O}^{t_j-t_{j-1}}$ for all $j \in [n_B]$, and $\bar{\mathbf{E}}(\mathbf{h}_1)$ is defined in (10). Then $\mathbf{U} := \text{BlkD}(\mathbf{U}_1, \dots, \mathbf{U}_{n_A})$ is an orthogonal matrix whose columns form an orthonormal basis for \mathbb{R}^d and $\bar{\mathbf{E}}(\mathbf{h}_1)$ selects t_{n_B} columns of \mathbf{U} .

Moreover, right multiplication by $\mathbf{\Pi}$ and $\text{BlkD}(\mathbf{V}_1^T, \dots, \mathbf{V}_{n_B}^T)$ does not change the column space of \mathbf{Q}_1 . Hence, with $\text{col}(\cdot)$ denoting the column space, $\text{col}(\mathbf{Q}_1) = \text{col}(\mathbf{U} \bar{\mathbf{E}}(\mathbf{h}_1))$. Since $\mathbf{Q} = [\mathbf{Q}_1, \mathbf{Q}_2] \in \text{St}(d, K)$, we have $\mathbf{Q}_1^T \mathbf{Q}_2 = \mathbf{0}$. Therefore, $\text{col}(\mathbf{Q}_2) \subseteq \text{col}(\mathbf{Q}_1)^\perp = \text{col}(\mathbf{U} \hat{\mathbf{E}}(\mathbf{h}_2))$. Hence, there exists $\mathbf{V}_{n_B+1} \in \text{St}(d-t_{n_B}, K-t_{n_B})$ such that $\mathbf{Q}_2 = \mathbf{U} \hat{\mathbf{E}}(\mathbf{h}_2) \mathbf{V}_{n_B+1}$. Consequently, \mathbf{Q} is in the form (12). \square

3 Optimization Landscape Analysis of QPOC

In this section, we study the optimization landscape of Problem (1). Without loss of generality, we focus on the case where \mathbf{B} is singular, since the nonsingular case corresponds to the special case $t_{n_B} = K$, where the zero block is absent. Moreover, for any scalar α , replacing \mathbf{A} in (6) by $\mathbf{A} + \alpha \mathbf{I}$ changes the objective value on $\text{St}(d, K)$ only by the additive constant $\alpha \text{Tr}(\mathbf{B})$. Therefore, we assume without loss of generality that $\mathbf{A} \succ \mathbf{0}$, i.e., $a_i > 0$ for all $i \in [d]$. To begin, we identify a condition, expressed in terms of the permutation and the signs of the nonzero diagonal entries of \mathbf{B} , under which a critical point is a global maximizer of Problem (1).

Before proceeding with the analysis, we introduce some notation. By Theorem 1, any

$\mathbf{Q} \in \mathcal{Q}_{\mathbf{h}, \mathbf{\Pi}}$ takes the form

$$\mathbf{Q} = \text{BlkD}(\mathbf{U}_1, \dots, \mathbf{U}_{n_A}) \begin{bmatrix} \bar{\mathbf{E}}(\mathbf{h}_1) \mathbf{\Pi} & \hat{\mathbf{E}}(\mathbf{h}_2) \mathbf{V}_{n_B+1} \end{bmatrix} \text{BlkD}(\mathbf{V}_1^T, \dots, \mathbf{V}_{n_B}^T, \mathbf{I}) \quad (13)$$

for some $\mathbf{U}_i \in \mathcal{O}^{s_i - s_{i-1}}$ for each $i \in [n_A]$, $\mathbf{V}_j \in \mathcal{O}^{t_j - t_{j-1}}$ for each $j \in [n_B]$, and $\mathbf{V}_{n_B+1} \in \text{St}(d - t_{n_B}, K - t_{n_B})$. For ease of exposition, define

$$\mathbf{U} := \text{BlkD}(\mathbf{U}_1, \dots, \mathbf{U}_{n_A}), \quad \mathbf{V} := \text{BlkD}(\mathbf{V}_1^T, \dots, \mathbf{V}_{n_B}^T, \mathbf{I}_{K-t_{n_B}}). \quad (14)$$

Moreover, define

$$\mathbf{\Psi} := \text{diag}(a_1, \dots, a_{t_p}, a_{d+t_p-t_{n_B}+1}, \dots, a_d) \in \mathbb{S}^{t_{n_B}}, \quad \forall p \in \{0, 1, \dots, n_B\}, \quad (15)$$

where the diagonal entries of $\mathbf{\Psi}$ are sorted in descending order. In particular, $p = 0$ (resp., $p = n_B$) indicates $\mathbf{\Psi} := \text{diag}(a_{d+1-t_{n_B}}, \dots, a_d)$ (resp., $\mathbf{\Psi} := \text{diag}(a_1, \dots, a_{t_p})$). Further define

$$\tilde{\mathbf{A}} := \mathbf{\Pi}^T \bar{\mathbf{E}}(\mathbf{h}_1)^T \mathbf{A} \bar{\mathbf{E}}(\mathbf{h}_1) \mathbf{\Pi} \in \mathbb{R}^{t_{n_B} \times t_{n_B}}. \quad (16)$$

Since \mathbf{A} is diagonal and $\bar{\mathbf{E}}(\mathbf{h}_1)$ is a coordinate-selection matrix, $\tilde{\mathbf{A}}$ is diagonal and admits the block partition

$$\tilde{\mathbf{A}} = \text{BlkD}(\text{diag}(\tilde{\mathbf{a}}_1), \dots, \text{diag}(\tilde{\mathbf{a}}_{n_B})), \quad \text{where } \tilde{\mathbf{a}}_i \in \mathbb{R}^{t_i - t_{i-1}}, \quad \forall i \in [n_B].$$

For each $i \in [n_B]$, choose $\bar{\mathbf{\Pi}}_i \in \mathcal{P}^{t_i - t_{i-1}}$ such that

$$\bar{\mathbf{\Pi}}_i^T \text{diag}(\tilde{\mathbf{a}}_i) \bar{\mathbf{\Pi}}_i = \text{diag}(\bar{\mathbf{a}}_i),$$

where $\bar{\mathbf{a}}_i = (\bar{a}_{i,1}, \dots, \bar{a}_{i,t_i - t_{i-1}})$ is sorted in decreasing order $\bar{a}_{i,1} \geq \bar{a}_{i,2} \geq \dots \geq \bar{a}_{i,t_i - t_{i-1}}$ for each $i \in [n_B]$. Let $\bar{\mathbf{\Pi}} := \text{BlkD}(\bar{\mathbf{\Pi}}_1, \dots, \bar{\mathbf{\Pi}}_{n_B})$ and

$$\mathbf{\Omega} := \text{BlkD}(\text{diag}(\bar{\mathbf{a}}_1), \dots, \text{diag}(\bar{\mathbf{a}}_{n_B})) = \bar{\mathbf{\Pi}}^T \tilde{\mathbf{A}} \bar{\mathbf{\Pi}}. \quad (17)$$

By construction, $\mathbf{\Omega}$ is a blockwise sorted version of $\tilde{\mathbf{A}}$, with the blocks corresponding to the equal-eigenvalue blocks of $\hat{\mathbf{B}}$ defined in (8). In contrast, $\mathbf{\Psi}$ represents the optimal spectral assignment dictated by the signs of the nonzero eigenvalues of \mathbf{B} : the positive entries of $\hat{\mathbf{B}}$ are paired with the largest diagonal entries of \mathbf{A} , whereas the negative entries are paired with the smallest ones. The following proposition shows that if this pattern is realized, then the corresponding critical point is globally optimal.

Proposition 1. *Fix $\mathbf{h} \in \tilde{\mathcal{H}}$ and $\mathbf{\Pi} \in \mathcal{P}^{t_{n_B}}$, and let $\mathbf{Q} \in \mathcal{Q}_{\mathbf{h}, \mathbf{\Pi}}$. Let $\mathbf{\Psi}$ and $\mathbf{\Omega}$ be defined as in (15) and (17), respectively. Suppose that $\mathbf{\Psi} = \mathbf{\Omega}$. Then \mathbf{Q} is a global maximizer.*

Proof. By Theorem 1, any $\mathbf{Q} \in \mathcal{Q}_{\mathbf{h}, \mathbf{\Pi}}$ takes the form (13). Define $\boldsymbol{\alpha} := \text{diag}(\bar{\mathbf{E}}(\mathbf{h}_1)^T \mathbf{A} \bar{\mathbf{E}}(\mathbf{h}_1)) \in \mathbb{R}^{t_{n_B}}$. Since \mathbf{A} is diagonal and $\bar{\mathbf{E}}(\mathbf{h}_1)$ is a coordinate-selection matrix, the entries of $\boldsymbol{\alpha}$ are precisely the t_{n_B} diagonal entries of \mathbf{A} selected by \mathbf{h}_1 . Substituting (13) into the objective of

Problem (1) gives

$$F(\mathbf{Q}) = \text{Tr} \left(\mathbf{\Pi}^T \bar{\mathbf{E}}(\mathbf{h}_1)^T \mathbf{A} \bar{\mathbf{E}}(\mathbf{h}_1) \mathbf{\Pi} \hat{\mathbf{B}} \right) = \text{Tr} \left(\mathbf{\Pi}^T \text{diag}(\boldsymbol{\alpha}) \mathbf{\Pi} \hat{\mathbf{B}} \right). \quad (18)$$

Thus, the value of $F(\mathbf{Q})$ depends only on the selected diagonal entries of \mathbf{A} , determined by \mathbf{h}_1 , and on their ordering, determined by $\mathbf{\Pi}$.

We next identify the largest possible value of (18). By the rearrangement inequality and the fact that all diagonal entries of \mathbf{A} are positive, this inner product is maximized by pairing the positive entries of $\hat{\mathbf{B}}$ with the largest t_p diagonal entries of \mathbf{A} and the negative entries with the smallest $t_{n_B} - t_p$ diagonal entries. Hence, for any feasible \mathbf{h}_1 and any permutation $\mathbf{\Pi}$,

$$F(\mathbf{Q}) \leq \sum_{i=1}^{t_p} a_i b_i + \sum_{i=t_p+1}^{t_{n_B}} a_{d-t_{n_B}+i} b_i. \quad (19)$$

It remains to show that \mathbf{Q} attains this upper bound. Since $\bar{\mathbf{\Pi}}$ only permutes coordinates within the equal-eigenvalue blocks of $\hat{\mathbf{B}}$, it commutes with $\hat{\mathbf{B}}$. Therefore, by cyclicity of the trace, (15–17), and $\boldsymbol{\Psi} = \boldsymbol{\Omega}$, we obtain

$$\begin{aligned} F(\mathbf{Q}) &= \text{Tr} \left(\mathbf{\Pi}^T \bar{\mathbf{E}}(\mathbf{h}_1)^T \mathbf{A} \bar{\mathbf{E}}(\mathbf{h}_1) \mathbf{\Pi} \hat{\mathbf{B}} \right) = \text{Tr} \left(\bar{\mathbf{\Pi}}^T \mathbf{\Pi}^T \bar{\mathbf{E}}(\mathbf{h}_1)^T \mathbf{A} \bar{\mathbf{E}}(\mathbf{h}_1) \mathbf{\Pi} \bar{\mathbf{\Pi}} \hat{\mathbf{B}} \right) \\ &= \text{Tr} \left(\boldsymbol{\Psi} \hat{\mathbf{B}} \right) = \sum_{i=1}^{t_p} a_i b_i + \sum_{i=t_p+1}^{t_{n_B}} a_{d-t_{n_B}+i} b_i. \end{aligned} \quad (20)$$

Thus \mathbf{Q} attains the upper bound in (19) and is therefore a global maximizer. \square

We next show that any critical point $\mathbf{Q} \in \mathcal{Q}_{\mathbf{h}, \mathbf{\Pi}}$ violating $\boldsymbol{\Psi} = \boldsymbol{\Omega}$ is a strict saddle point. The proof is to construct an ascent direction along which the Riemannian Hessian has positive curvature. This relies on Givens rotations [11].

Definition 2 (Givens rotations). Given a positive integer n , for any indices $1 \leq i \neq j \leq n$ and angle $\theta \in \mathbb{R}$, the Givens rotation matrix $\mathbf{G}(i, j, \theta) \in \mathbb{R}^{n \times n}$ is defined as the identity matrix except for the 2×2 block indexed by rows and columns (i, j) , where $g_{ii} = \cos \theta$, $g_{ij} = \sin \theta$, $g_{ji} = -\sin \theta$, $g_{jj} = \cos \theta$.

The next lemma provides an elementary identity that can be verified by a direct expansion of the affected (i, j) block.

Lemma 1. Let $\mathbf{C} = \text{diag}(c_1, \dots, c_n)$ and $\mathbf{D} = \text{diag}(d_1, \dots, d_n)$ be diagonal matrices. Then it holds that

$$\text{Tr} \left(\mathbf{G}(i, j, \theta)^T \mathbf{D} \mathbf{G}(i, j, \theta) \mathbf{C} \right) - \text{Tr}(\mathbf{D} \mathbf{C}) = (c_j - c_i)(d_i - d_j) \sin^2 \theta.$$

We next present a counting lemma that identifies a useful mismatched coordinate for the subsequent construction of an improving rotation direction.

Lemma 2. Suppose that $\boldsymbol{\Omega} \neq \boldsymbol{\Psi}$, where $\boldsymbol{\Psi}$ and $\boldsymbol{\Omega}$ are defined in (15) and (17), respectively. Write $\omega_i := \boldsymbol{\Omega}(i, i)$ and $\psi_i := \boldsymbol{\Psi}(i, i)$ for $i \in [t_{n_B}]$. If $\omega_i \neq \psi_i$ for some $i \leq t_p$, let $i^* := \min\{i \leq$

$t_p : \omega_i \neq \psi_i$; otherwise, let $i^* := \max\{i > t_p : \omega_i \neq \psi_i\}$. Then, we have

$$i^* \leq t_p \Rightarrow \omega_{i^*} < \psi_{i^*}, \quad i^* > t_p \Rightarrow \omega_{i^*} > \psi_{i^*}.$$

Moreover, let $k \in [n_A]$ be such that $\psi_{i^*} = a_{s_{k-1}+1} = \dots = a_{s_k}$. If $\omega_j \neq \psi_{i^*}$ for all $j > i^*$ when $i^* \leq t_p$, or $\omega_j \neq \psi_{i^*}$ for all $j < i^*$ when $i^* > t_p$, then $h_{2,k} > 0$.

Proof. We first consider the case $i^* \leq t_p$. By the definition of i^* , $\omega_i = \psi_i$ for all $i < i^*$. Since $\psi_1, \dots, \psi_{t_p}$ are the largest t_p diagonal entries of \mathbf{A} in nonincreasing order, all diagonal entries of \mathbf{A} that are strictly larger than ψ_{i^*} appear among $\psi_1, \dots, \psi_{i^*-1}$. Hence, if $\omega_{i^*} > \psi_{i^*}$, then the number of entries strictly larger than ψ_{i^*} in $\omega_1, \dots, \omega_{i^*}$ would exceed the corresponding multiplicity in the spectrum of \mathbf{A} , a contradiction. Since $\omega_{i^*} \neq \psi_{i^*}$, we obtain $\omega_{i^*} < \psi_{i^*}$. The case $i^* > t_p$ is analogous.

It remains to prove the last assertion. We argue by contradiction. Set $m_k := s_k - s_{k-1}$. Suppose, to the contrary, that $h_{2,k} = 0$. Since $h_{1,k} + h_{2,k} = m_k$, all m_k copies of the eigenvalue ψ_{i^*} are selected by $\bar{\mathbf{E}}(\mathbf{h}_1)$. Hence $\mathbf{\Omega}$, which is obtained by sorting the selected diagonal entries blockwise, must contain exactly m_k diagonal entries equal to ψ_{i^*} .

Consider the case $i^* \leq t_p$. Since $\omega_i = \psi_i$ for all $i < i^*$ and $\psi_{i^*} = \psi_{i^*}$, we have $|\{i < i^* : \omega_i = \psi_{i^*}\}| = |\{i < i^* : \psi_i = \psi_{i^*}\}| \leq m_k - 1$. Moreover, $\omega_{i^*} \neq \psi_{i^*}$. Hence, if no $j > i^*$ satisfies $\omega_j = \psi_{i^*}$, then the diagonal entries of $\mathbf{\Omega}$ contain at most $m_k - 1$ copies of ψ_{i^*} , contradicting $h_{2,k} = 0$. Therefore $h_{2,k} > 0$. The case $i^* > t_p$ is analogous, with the order reversed. \square

Based on the above setup, we now construct an ascent direction for each critical point that does not satisfy $\mathbf{\Psi} = \mathbf{\Omega}$ in the following proposition.

Proposition 2. *Let $\mathbf{h} \in \tilde{\mathcal{H}}$, $\mathbf{\Pi} \in \mathcal{P}^{t_{n_B}}$, and $\mathbf{Q} \in \mathcal{Q}_{\mathbf{h}, \mathbf{\Pi}}$ be arbitrary. Let $\mathbf{\Psi}$ and $\mathbf{\Omega}$ be defined as in (15) and (17), respectively. Suppose that $\mathbf{\Psi} \neq \mathbf{\Omega}$. Then \mathbf{Q} is a strict saddle point.*

Proof. Let π and $\bar{\pi}$ denote the permutations induced by $\mathbf{\Pi}$ and $\bar{\mathbf{\Pi}}$, respectively. By assumption, $\mathbf{\Omega} \neq \mathbf{\Psi}$. Write $\omega_i := \mathbf{\Omega}(i, i)$ and $\psi_i := \mathbf{\Psi}(i, i)$ for $i \in [t_{n_B}]$. Choose i^* as in Lemma 2: if a mismatch occurs among the first t_p entries, set $i^* := \min\{i \leq t_p : \omega_i \neq \psi_i\}$; otherwise, set $i^* := \max\{i > t_p : \omega_i \neq \psi_i\}$. We distinguish two cases according to whether the value ψ_{i^*} appears on the opposite side of i^* in $\mathbf{\Omega}$.

Case 1: Either $i^* \leq t_p$ and there exists $j > i^*$ such that $\omega_j = \psi_{i^*}$, or $i^* > t_p$ and there exists $j < i^*$ such that $\omega_j = \psi_{i^*}$. If $i^* \leq t_p$, then by Lemma 2, $\omega_{i^*} < \psi_{i^*} = \omega_j$. Since $j > i^*$ and the diagonal entries of $\hat{\mathbf{B}}$ are nonincreasing, it suffices to rule out the possibility that $b_{i^*} = b_j$. If $b_{i^*} = b_j$, then i^* and j belong to the same equal-eigenvalue block of $\hat{\mathbf{B}}$. This contradicts $\omega_{i^*} < \omega_j$, since $\mathbf{\Omega}$ is sorted in nonincreasing order within each block. Therefore, $b_{i^*} > b_j$. If $i^* > t_p$, then by Lemma 2, $\omega_{i^*} > \psi_{i^*} = \omega_j$. A similar argument gives $b_j > b_{i^*}$. Therefore, in both situations, we have

$$(b_j - b_{i^*})(\omega_{i^*} - \omega_j) > 0. \quad (21)$$

Set $i' := \bar{\pi}^{-1}(i^*)$ and $j' := \bar{\pi}^{-1}(j)$. Since $\bar{\mathbf{\Pi}}$ is block diagonal with respect to the equal-eigenvalue blocks of $\hat{\mathbf{B}}$, we have $b_{i'} = b_{i^*}$ and $b_{j'} = b_j$. Moreover, by (17),

$$\tilde{\mathbf{A}}(i', i') = \omega_{i^*}, \quad \tilde{\mathbf{A}}(j', j') = \omega_j. \quad (22)$$

Moreover, we define $\mathbf{G}(\theta) := \mathbf{G}(i', j', \theta) \in \mathbb{R}^{t_{n_B} \times t_{n_B}}$ and the Stiefel trajectory

$$\mathbf{Q}(\theta) := U \left[\bar{\mathbf{E}}(\mathbf{h}_1) \mathbf{\Pi} \mathbf{G}(\theta) \quad \hat{\mathbf{E}}(\mathbf{h}_2) \mathbf{V}_{n_B+1} \right] \mathbf{V}.$$

Obviously, $\mathbf{Q}(0) = \mathbf{Q}$ due to $\mathbf{G}(0) = \mathbf{I}$, (13), and (14), and $\mathbf{Q}(\theta) \in \text{St}(d, K)$. Moreover, for a sufficiently small $\theta \neq 0$, we obtain

$$\begin{aligned} F(\mathbf{Q}(\theta)) - F(\mathbf{Q}) &= \text{Tr}(\mathbf{Q}(\theta)^T \mathbf{A} \mathbf{Q}(\theta) \mathbf{B}) - \text{Tr}(\mathbf{Q}^T \mathbf{A} \mathbf{Q} \mathbf{B}) \\ &= \text{Tr}(\mathbf{G}(\theta)^T \tilde{\mathbf{A}} \mathbf{G}(\theta) \tilde{\mathbf{B}}) - \text{Tr}(\tilde{\mathbf{A}} \tilde{\mathbf{B}}) \\ &= (b_{j'} - b_{i'}) \left(\tilde{\mathbf{A}}(i', i') - \tilde{\mathbf{A}}(j', j') \right) \sin^2 \theta \\ &= (b_j - b_{i^*}) (\omega_{i^*} - \omega_j) \sin^2 \theta > 0, \end{aligned}$$

where the second equality uses (14), (8), and (16), the third equality uses Lemma 1 with $\mathbf{D} = \tilde{\mathbf{A}}$ and $\mathbf{C} = \tilde{\mathbf{B}}$, the last equality uses (22), and the inequality follows from (21). Let $\mathbf{D} := \mathbf{Q}'(0) \in \text{T}(\mathbf{Q})$. Since $\sin^2 \theta = \theta^2 + o(\theta^2)$ and \mathbf{Q} is critical, the standard second-derivative formula on the Stiefel manifold [3, (5.26), p. 107] yields $\langle \mathbf{D}, \text{Hess } F(\mathbf{Q})[\mathbf{D}] \rangle > 0$. Hence \mathbf{Q} is a strict saddle point.

Case 2: Case 1 does not occur. Choose $k \in [n_A]$ such that $\psi_{i^*} = a_{s_{k-1}+1} = \dots = a_{s_k}$. Then there is no $j > i^*$ with $\omega_j = \psi_{i^*}$ if $i^* \leq t_p$, and no $j < i^*$ with $\omega_j = \psi_{i^*}$ if $i^* > t_p$. Hence Lemma 2 gives $h_{2,k} > 0$. Choose the last column of $\hat{\mathbf{E}}_k(\mathbf{h}_2)$, i.e., let $g_k := \sum_{i=1}^k h_{2,i}$. Then $\hat{\mathbf{E}}(\mathbf{h}_2) \mathbf{e}_{g_k}$ lies in the k -th eigenspace of \mathbf{A} .

Let $i' := \bar{\pi}^{-1}(i^*)$, so i' and i^* lie in the same block of (17) and hence $b_{i^*} = b_{i'}$. By Lemma 2, if $i^* \leq t_p$ then $b_{i'} > 0$ and $\psi_{i^*} > \omega_{i^*}$, while if $i^* > t_p$ then $b_{i'} < 0$ and $\psi_{i^*} < \omega_{i^*}$. Then we have

$$b_{i'} (\psi_{i^*} - \omega_{i^*}) > 0. \quad (23)$$

Set $\mathbf{u} := \bar{\mathbf{E}}(\mathbf{h}_1) \mathbf{e}_{\pi^{-1}(i')}$ and $\mathbf{v} := \hat{\mathbf{E}}(\mathbf{h}_2) \mathbf{e}_{g_k}$. Then

$$\mathbf{u}^T \mathbf{A} \mathbf{u} = \tilde{\mathbf{A}}(i', i') = \omega_{i^*}, \quad \mathbf{v}^T \mathbf{A} \mathbf{v} = a_{s_k} = \psi_{i^*},$$

where the identities for \mathbf{u} follow from (16), (17), and the choice $i' = \bar{\pi}^{-1}(i^*)$, while the identity for \mathbf{v} follows from the choice of g_k . For $\theta \in \mathbb{R}$, define $\bar{\mathbf{E}}(\mathbf{h}_1, \theta)$ and $\hat{\mathbf{E}}(\mathbf{h}_2, \theta)$ by changing only the $\pi^{-1}(i')$ -th column of $\bar{\mathbf{E}}(\mathbf{h}_1)$ and the g_k -th column of $\hat{\mathbf{E}}(\mathbf{h}_2)$ as follows:

$$\bar{\mathbf{E}}(\mathbf{h}_1, \theta)_{:, \pi^{-1}(i')} = \mathbf{u} \cos \theta + \mathbf{v} \sin \theta, \quad \hat{\mathbf{E}}(\mathbf{h}_2, \theta)_{:, g_k} = -\mathbf{u} \sin \theta + \mathbf{v} \cos \theta,$$

with all other columns unchanged. Let

$$\mathbf{Q}(\theta) := U \left[\bar{\mathbf{E}}(\mathbf{h}_1, \theta) \mathbf{\Pi} \quad \hat{\mathbf{E}}(\mathbf{h}_2, \theta) \mathbf{V}_{n_B+1} \right] \mathbf{V}.$$

By (13) and (14), $\mathbf{Q}(0) = \mathbf{Q}$. Since the two changed columns are obtained by an orthogonal rotation of the orthonormal pair \mathbf{u}, \mathbf{v} , we also have $\mathbf{Q}(\theta) \in \text{St}(d, K)$. Using (8), (13), (14), and

the fact that the zero block of \mathbf{B} contributes nothing, the objective function can be written as

$$F(\mathbf{Q}(\theta)) = \sum_{l=1}^{t_{n_B}} b_l \left[(\bar{\mathbf{E}}(\mathbf{h}_1, \theta) \mathbf{e}_{\pi^{-1}(l)})^T \mathbf{A} (\bar{\mathbf{E}}(\mathbf{h}_1, \theta) \mathbf{e}_{\pi^{-1}(l)}) \right].$$

Since only the $\pi^{-1}(i')$ -th column of $\bar{\mathbf{E}}(\mathbf{h}_1)$ is changed among the selected columns, all terms with $l \neq i'$ cancel in $F(\mathbf{Q}(\theta)) - F(\mathbf{Q})$. Hence, for sufficiently small $\theta \neq 0$,

$$\begin{aligned} F(\mathbf{Q}(\theta)) - F(\mathbf{Q}) &= b_{i'} [(\mathbf{u} \cos \theta + \mathbf{v} \sin \theta)^T \mathbf{A} (\mathbf{u} \cos \theta + \mathbf{v} \sin \theta) - \mathbf{u}^T \mathbf{A} \mathbf{u}] \\ &= b_{i'} [\mathbf{u}^T \mathbf{A} \mathbf{u} (\cos^2 \theta - 1) + \mathbf{v}^T \mathbf{A} \mathbf{v} \sin^2 \theta] \\ &= b_{i'} (\psi_{i^*} - \omega_{i^*}) \sin^2 \theta > 0, \end{aligned}$$

where the second equality uses $\mathbf{u}^T \mathbf{A} \mathbf{v} = 0$, and the last inequality follows from (23). As in Case 1, setting $\mathbf{D} := \mathbf{Q}'(0) \in \mathbb{T}(\mathbf{Q})$ and using $\sin^2 \theta = \theta^2 + o(\theta^2)$, together with the criticality of \mathbf{Q} , yields $\langle \mathbf{D}, \text{Hess } F(\mathbf{Q})[\mathbf{D}] \rangle > 0$. Thus \mathbf{Q} is a strict saddle point. \square

Building on Lemmas 1 and 2 and Propositions 1 and 2, we obtain the following result directly.

Theorem 2 (Benign optimization landscape of QPOC). *Let $\mathbf{h} \in \tilde{\mathcal{H}}$, $\mathbf{\Pi} \in \mathcal{P}^{t_{n_B}}$, and $\mathbf{Q} \in \mathcal{Q}_{\mathbf{h}, \mathbf{\Pi}}$ be arbitrary. Let Ψ and Ω be defined as in (15) and (17), respectively. Suppose that $\Psi = \Omega$. Then \mathbf{Q} is a global maximizer. Otherwise, \mathbf{Q} is a strict saddle point.*

We close this section with two comments. First, Theorem 2 gives an exact classification of all critical points of Problem (1): the condition $\Psi = \Omega$ characterizes global maximizers, while every other critical point is a strict saddle point. Hence Problem (1) has a benign optimization landscape. Second, combined with strict-saddle avoidance for randomly initialized first-order methods [16] and the Lojasiewicz exponent 1/2 for Problem (1) [20], this result provides a theoretical explanation for the observed convergence of retraction-based gradient methods to global maximizers at a local linear rate. The same conclusion extends to the general symmetric case by orthogonally diagonalizing \mathbf{B} , grouping its nonzero eigenvalues by sign, and applying the shift $\mathbf{A} \mapsto \mathbf{A} + \alpha \mathbf{I}$ for some scalar α . If $\mathbf{B} = \mathbf{0}$ or $\mathbf{A} = \alpha \mathbf{I}_d$ for some scalar α , the objective is constant on $\text{St}(d, K)$, and every feasible point is a global maximizer.

4 Application to Heteroscedastic Probabilistic PCA

In this section, we apply the optimization landscape characterization of Problem (1) to HePPCA. After introducing the model in Section 4.1, we use the QPOC formulation of the population HePPCA problem from [25] to establish its benign landscape in Section 4.2. We then show in Section 4.3 that this benign landscape persists for the empirical problem under mild conditions.

4.1 Problem Setup

Consider the HePPCA problem with L data groups, where the l -th group contains n_l samples for each $l \in [L]$. For ease of exposition, let $n := \sum_{l=1}^L n_l$ and denote the i -th sample in the l -th

group by $\mathbf{y}_{l,i} \in \mathbb{R}^d$. The samples $\{\mathbf{y}_{l,i}\} \subseteq \mathbb{R}^d$ are generated according to the model

$$\mathbf{y}_{l,i} = \mathbf{Q}^* \text{diag}(\sqrt{\boldsymbol{\lambda}}) \mathbf{z}_{l,i} + \boldsymbol{\delta}_{l,i}, \quad \forall l \in [L], i \in [n_l], \quad (24)$$

where $\mathbf{Q}^* \in \text{St}(d, K)$ denotes the ground-truth subspace to be estimated, $\boldsymbol{\lambda} = (\lambda_1, \dots, \lambda_K)$ with $\lambda_1 > \dots > \lambda_K > 0$ denotes the signal strengths, $\mathbf{z}_{l,i} \stackrel{i.i.d.}{\sim} \mathcal{N}(\mathbf{0}, \mathbf{I}_K)$ are latent variables, and $\boldsymbol{\delta}_{l,i} \sim \mathcal{N}(\mathbf{0}, v_l \mathbf{I}_d)$ are additive heteroscedastic noise terms with $v_l > 0$. We assume that the noise terms are independent across all samples and independent of all latent variables. In this work, we assume that the signal and noise strengths are known. We note that [13] provides a practical procedure for estimating these parameters from observed data.

According to [9, 13], a maximum likelihood estimator of the ground-truth subspace \mathbf{Q}^* can be obtained by solving the following non-convex problem:

$$\max_{\mathbf{Q} \in \mathbb{R}^{d \times K}} F(\mathbf{Q}) := \sum_{k=1}^K \mathbf{q}_k^T \mathbf{A}_k \mathbf{q}_k \quad \text{s.t.} \quad \mathbf{Q} \in \text{St}(d, K), \quad (25)$$

where \mathbf{q}_k denotes the k -th column of \mathbf{Q} , $\mathbf{Y}_l = [\mathbf{y}_{l,1}, \dots, \mathbf{y}_{l,n_l}] \in \mathbb{R}^{d \times n_l}$ for all $l \in [L]$, and

$$w_{l,k} := \frac{\lambda_k}{\lambda_k + v_l}, \quad \mathbf{A}_k := \sum_{l=1}^L \frac{w_{l,k}}{n v_l} \mathbf{Y}_l \mathbf{Y}_l^T. \quad (26)$$

Using the data model above, the expectation of \mathbf{A}_k is given as follows, whose proof is provided in [25, Lemma 1].

Lemma 3. *For each $k \in [K]$, it holds that*

$$\mathbb{E}[\mathbf{A}_k] = \left(\sum_{l=1}^L \frac{w_{l,k} n_l}{n v_l} \right) \mathbf{Q}^* \text{diag}(\boldsymbol{\lambda}) \mathbf{Q}^{*T} + \left(\sum_{l=1}^L \frac{w_{l,k} n_l}{n} \right) \mathbf{I}_d. \quad (27)$$

4.2 Benign Optimization Landscape of Population HePPCA

Replacing each \mathbf{A}_k in Problem (25) with its expectation $\mathbb{E}[\mathbf{A}_k]$ and dropping the resulting additive constant, define $\mathbf{w} := (w_1, \dots, w_K)$ with $w_k := \sum_{l=1}^L \frac{n_l w_{l,k}}{n v_l}$, and let

$$\mathbf{W} := \text{diag}(\mathbf{w}), \quad \boldsymbol{\Lambda} := \text{diag}(\boldsymbol{\lambda}).$$

Then we obtain the following population objective:

$$\max_{\mathbf{Q} \in \mathbb{R}^{d \times K}} G(\mathbf{Q}) := \text{Tr}(\mathbf{Q}^T \mathbf{Q}^* \boldsymbol{\Lambda} \mathbf{Q}^{*T} \mathbf{Q} \mathbf{W}) \quad \text{s.t.} \quad \mathbf{Q} \in \text{St}(d, K). \quad (28)$$

It follows from $\lambda_1 > \dots > \lambda_K$ and (26) that $w_1 > \dots > w_K$. We denote the critical point set of Problem (28) by

$$\mathcal{Q}_G := \{\mathbf{Q} \in \text{St}(d, K) : \text{grad } G(\mathbf{Q}) = \mathbf{0}\}.$$

Thus, Problem (28) is a special case of Problem (1). Moreover, let $\bar{\mathbf{Q}}^* \in \mathbb{R}^{d \times (d-K)}$ be any matrix such that $[\mathbf{Q}^* \ \bar{\mathbf{Q}}^*] \in \mathcal{O}^d$. Then $\mathbf{Q}^* \boldsymbol{\Lambda} \mathbf{Q}^{*T}$ admits the eigen-decomposition

$$\mathbf{Q}^* \boldsymbol{\Lambda} \mathbf{Q}^{*T} = \begin{bmatrix} \mathbf{Q}^* & \bar{\mathbf{Q}}^* \end{bmatrix} \begin{bmatrix} \boldsymbol{\Lambda} & \mathbf{0} \\ \mathbf{0} & \mathbf{0} \end{bmatrix} \begin{bmatrix} \mathbf{Q}^* & \bar{\mathbf{Q}}^* \end{bmatrix}^T.$$

Using this decomposition, $\lambda_1 > \dots > \lambda_K > 0$, and Fact 1, one can verify that the critical point set of Problem (28) can be expressed as follows. Define

$$\mathcal{H}_G := \left\{ (h_1, \dots, h_{K+1}) : \sum_{i=1}^{K+1} h_i = K, h_i \in \{0, 1\}, \forall i \in [K], h_{K+1} \in \{0, 1, \dots, d-K\} \right\}.$$

In addition, for any $\mathbf{h} = (h_1, \dots, h_K, h_{K+1}) \in \mathcal{H}_G$, we define $\mathbf{E}(\mathbf{h}) \in \mathbb{R}^{d \times K}$ by $\mathbf{E}(\mathbf{h}) := [\mathbf{E}_1(\mathbf{h}) \ \dots \ \mathbf{E}_K(\mathbf{h}) \ \mathbf{E}_{K+1}(\mathbf{h})]$, where for each $i \in [K]$,

$$\mathbf{E}_i(\mathbf{h}) := \begin{cases} \mathbf{e}_i, & \text{if } h_i = 1, \\ \emptyset, & \text{if } h_i = 0, \end{cases} \quad \mathbf{E}_{K+1}(\mathbf{h}) := \begin{cases} [\mathbf{e}_{K+1} \ \dots \ \mathbf{e}_{K+h_{K+1}}], & \text{if } h_{K+1} \neq 0, \\ \emptyset, & \text{if } h_{K+1} = 0. \end{cases}$$

Here, \emptyset denotes an empty matrix of size $d \times 0$, which is omitted from the concatenation, and $\{\mathbf{e}_i\}_{i=1}^d \subseteq \mathbb{R}^d$ is the standard basis of \mathbb{R}^d . Using Fact 1 and the setup above, one can verify the following closed-form expression for the critical point set of Problem (28).

Proposition 3. *It holds that $\mathcal{Q}_G = \bigcup_{\mathbf{h} \in \mathcal{H}_G, \mathbf{\Pi} \in \mathcal{P}^K} \mathcal{Q}_{\mathbf{h}, \mathbf{\Pi}}$, where every $\mathbf{Q} \in \mathcal{Q}_{\mathbf{h}, \mathbf{\Pi}}$ takes the form*

$$\mathbf{Q} = [\mathbf{Q}^* \ \bar{\mathbf{Q}}^*] \text{BlkD}(\text{diag}(\mathbf{s}), \mathbf{S}_{K+1}) \mathbf{E}(\mathbf{h}) \cdot \mathbf{\Pi} \cdot \text{diag}(\mathbf{t}) \quad (29)$$

for some $\mathbf{s}, \mathbf{t} \in \mathbb{R}^K$ with $s_i, t_i \in \{1, -1\}$ for each $i \in [K]$ and $\mathbf{S}_{K+1} \in \mathcal{O}^{d-K}$.

Proof. Let $\mathbf{U}_* := [\mathbf{Q}^* \ \bar{\mathbf{Q}}^*] \in \mathcal{O}^d$ and set $\tilde{\mathbf{Q}} := \mathbf{U}_*^T \mathbf{Q}$. The map $\mathbf{Q} \mapsto \mathbf{U}_*^T \mathbf{Q}$ is a bijection from $\text{St}(d, K)$ onto itself. Hence \mathbf{Q} is a critical point of the population problem if and only if $\tilde{\mathbf{Q}}$ is a critical point of the diagonal QPOC

$$\max_{\tilde{\mathbf{Q}} \in \mathbb{R}^{d \times K}} \text{Tr} \left(\tilde{\mathbf{Q}}^T \text{BlkD}(\boldsymbol{\Lambda}, \mathbf{0}) \tilde{\mathbf{Q}} \mathbf{W} \right) \quad \text{s.t.} \quad \tilde{\mathbf{Q}} \in \text{St}(d, K). \quad (30)$$

Since $\lambda_1 > \dots > \lambda_K > 0$ and $w_1 > \dots > w_K > 0$, applying Fact 1 to (30) gives

$$\tilde{\mathbf{Q}} = \text{BlkD}(\text{diag}(\mathbf{s}), \mathbf{S}_{K+1}) \mathbf{E}(\mathbf{h}) \mathbf{\Pi} \text{diag}(\mathbf{t}),$$

where $\mathbf{h} \in \mathcal{H}_G$, $\mathbf{\Pi} \in \mathcal{P}^K$, $s_i, t_i \in \{1, -1\}$ for $i \in [K]$, and $\mathbf{S}_{K+1} \in \mathcal{O}^{d-K}$. Substituting this into $\mathbf{Q} = \mathbf{U}_* \tilde{\mathbf{Q}}$ gives (29). The converse inclusion follows from the same characterization in Fact 1. Hence the stated representation of \mathcal{Q}_G holds. \square

We next show that, for fixed $\mathbf{h} \in \mathcal{H}_G$ and $\mathbf{\Pi} \in \mathcal{P}^K$, all points in $\mathcal{Q}_{\mathbf{h}, \mathbf{\Pi}}$ have the same type of criticality.

Lemma 4. Let $\mathbf{h} \in \mathcal{H}_G$ and $\mathbf{\Pi} \in \mathcal{P}^K$ be arbitrary, and let $\mathbf{Q}, \widehat{\mathbf{Q}} \in \mathcal{Q}_{\mathbf{h}, \mathbf{\Pi}}$. Then \mathbf{Q} is a local minimizer, local maximizer, global minimizer, global maximizer, or strict saddle point if and only if $\widehat{\mathbf{Q}}$ has the same classification.

Proof. By Proposition 3, \mathbf{Q} can be written in the form (29) for some $\mathbf{s}, \mathbf{t} \in \mathbb{R}^K$ with $s_i, t_i \in \{1, -1\}$ for each $i \in [K]$ and some $\mathbf{S}_{K+1} \in \mathcal{O}^{d-K}$. Set $\mathbf{Q}' := [\mathbf{Q}^* \bar{\mathbf{Q}}^*] \mathbf{E}(\mathbf{h}) \mathbf{\Pi}$. Define the linear mapping ψ by

$$\psi(\mathbf{Z}) := [\mathbf{Q}^* \bar{\mathbf{Q}}^*] \text{BlkD}(\text{diag}(\mathbf{s}), \mathbf{S}_{K+1}) [\mathbf{Q}^* \bar{\mathbf{Q}}^*]^T \mathbf{Z} \text{diag}(\mathbf{t}).$$

Then $\psi(\mathbf{Q}') = \mathbf{Q}$. Moreover, since the matrices multiplying \mathbf{Z} from the left and right are orthogonal, ψ is an isometric bijection from $\text{St}(d, K)$ onto itself.

Now, we verify that $G(\psi(\mathbf{Z})) = G(\mathbf{Z})$ holds for all \mathbf{Z} :

$$\begin{aligned} G(\psi(\mathbf{Z})) &= \text{Tr}(\psi(\mathbf{Z})^T \mathbf{Q}^* \mathbf{\Lambda} \mathbf{Q}^{*T} \psi(\mathbf{Z}) \mathbf{W}) \\ &= \text{Tr}(\psi(\mathbf{Z})^T [\mathbf{Q}^* \bar{\mathbf{Q}}^*] \text{BlkD}(\mathbf{\Lambda}, \mathbf{0}) [\mathbf{Q}^* \bar{\mathbf{Q}}^*]^T \psi(\mathbf{Z}) \mathbf{W}) \\ &= \text{Tr}(\text{diag}(\mathbf{t}) \mathbf{Z}^T [\mathbf{Q}^* \bar{\mathbf{Q}}^*] \text{BlkD}(\text{diag}(\mathbf{s}), \mathbf{S}_{K+1}^T) \text{BlkD}(\mathbf{\Lambda}, \mathbf{0}) \\ &\quad \text{BlkD}(\text{diag}(\mathbf{s}), \mathbf{S}_{K+1}) [\mathbf{Q}^* \bar{\mathbf{Q}}^*]^T \mathbf{Z} \text{diag}(\mathbf{t}) \mathbf{W}) \\ &= \text{Tr}(\mathbf{Z}^T [\mathbf{Q}^* \bar{\mathbf{Q}}^*] \text{BlkD}(\mathbf{\Lambda}, \mathbf{0}) [\mathbf{Q}^* \bar{\mathbf{Q}}^*]^T \mathbf{Z} \mathbf{W}) = G(\mathbf{Z}), \end{aligned}$$

where the fourth equality uses $s_i, t_i \in \{1, -1\}$ for each $i \in [K]$.

Since ψ is an isometry of $\text{St}(d, K)$ and $G \circ \psi = G$, it preserves local and global optimality. Moreover, since ψ is a Riemannian isometry and $G \circ \psi = G$, the Riemannian Hessian quadratic form is invariant under ψ . Indeed, for any geodesic γ with $\gamma(0) = \mathbf{Z}$ and $\gamma'(0) = \mathbf{D}$, the curve $\psi \circ \gamma$ is a geodesic with initial velocity $\text{D}\psi(\mathbf{Z})[\mathbf{D}]$, and $G(\psi(\gamma(t))) = G(\gamma(t))$. Taking second derivatives at $t = 0$ gives the claim. Applying the same argument to $\widehat{\mathbf{Q}}$ gives the claim. \square

Using this lemma, to determine the type of each critical point in $\mathcal{Q}_{\mathbf{h}, \mathbf{\Pi}}$, it suffices to study the representative $\mathbf{Q} \in \mathcal{Q}_{\mathbf{h}, \mathbf{\Pi}}$ of the form

$$\mathbf{Q} = [\mathbf{Q}^* \bar{\mathbf{Q}}^*] \cdot \mathbf{E}(\mathbf{h}) \cdot \mathbf{\Pi}. \quad (31)$$

Using Theorem 2, we directly obtain the optimization landscape of Problem (28) and explicitly characterize its set of global maximizers as follows.

Proposition 4. Each critical point of Problem (28) is either a global maximizer or a strict saddle point. In particular, the set of global maximizers is

$$\mathcal{Q}_{\text{opt}} := \{\mathbf{Q}^* \text{diag}(\mathbf{s}) : s_i \in \{1, -1\}, i \in [K]\}. \quad (32)$$

Proof. The first statement follows from Theorem 2. It remains to characterize the global maximizers. By Lemma 4, it suffices to consider (31). Let $\boldsymbol{\mu} := (\lambda_1, \dots, \lambda_K, 0, \dots, 0) \in \mathbb{R}^d$. For any $\mathbf{h} \in \mathcal{H}_G$ and $\mathbf{\Pi} \in \mathcal{P}^K$, substituting (31) into (28) yields

$$G(\mathbf{Q}) = \text{Tr}(\mathbf{\Pi}^T \mathbf{E}^T(\mathbf{h}) \text{diag}(\boldsymbol{\mu}) \mathbf{E}(\mathbf{h}) \mathbf{\Pi} \mathbf{W}).$$

Since $\lambda_1 > \dots > \lambda_K > 0$ and $w_1 > \dots > w_K > 0$, the rearrangement inequality implies $G(\mathbf{Q}) \leq \sum_{k=1}^K \lambda_k w_k$, and equality holds for (31) if and only if $\mathbf{E}(\mathbf{h})\mathbf{\Pi} = \begin{bmatrix} \mathbf{I}_K & \mathbf{0} \end{bmatrix}^T$. Substituting this condition into (29), we obtain $\mathbf{Q} = \mathbf{Q}^* \text{diag}(\mathbf{s}) \text{diag}(\mathbf{t})$. Since $s_i, t_i \in \{1, -1\}$ for each $i \in [K]$, this is equivalent to the form in (32). \square

Building on Theorem 2 and Proposition 4, we further show that the population objective has a negative-definite Riemannian Hessian at every global maximizer and a positive-curvature direction at every other critical point.

Proposition 5. *The following hold for the objective G in Problem (28):*

(i) *There exists $\delta_1 > 0$ such that, for every $\mathbf{Q} \in \mathcal{Q}_{\text{opt}}$ and every $\mathbf{D} \in \mathbb{T}(\mathbf{Q})$,*

$$\langle \mathbf{D}, \text{Hess } G(\mathbf{Q})[\mathbf{D}] \rangle \leq -\delta_1 \|\mathbf{D}\|_F^2. \quad (33)$$

(ii) *There exists $\delta_2 > 0$ such that, for every $\mathbf{Q} \in \mathcal{Q}_G \setminus \mathcal{Q}_{\text{opt}}$, there exists a nonzero $\mathbf{D} \in \mathbb{T}(\mathbf{Q})$ satisfying*

$$\langle \mathbf{D}, \text{Hess } G(\mathbf{Q})[\mathbf{D}] \rangle \geq \delta_2 \|\mathbf{D}\|_F^2. \quad (34)$$

Proof. (i) It suffices to consider $\mathbf{Q} = \mathbf{Q}^*$, since the map $\mathbf{Q} \mapsto \mathbf{Q} \text{diag}(\mathbf{s})$ is an isometry on $\text{St}(d, K)$ and leaves G invariant for any $\mathbf{s} \in \{1, -1\}^K$.

For any direction $\mathbf{D} \in \mathbb{T}(\mathbf{Q}^*)$, decompose it as

$$\mathbf{D} = \underbrace{(\mathbf{I} - \mathbf{Q}^* \mathbf{Q}^{*T}) \mathbf{D}}_{\mathbf{D}_1} + \underbrace{\mathbf{Q}^* \mathbf{Q}^{*T} \mathbf{D}}_{\mathbf{D}_2}.$$

Let $\widehat{\mathbf{D}} := \mathbf{Q}^{*T} \mathbf{D}$. Since $\mathbf{D} \in \mathbb{T}(\mathbf{Q}^*)$, $\widehat{\mathbf{D}}$ is skew-symmetric and $\mathbf{D}_2 = \mathbf{Q}^* \widehat{\mathbf{D}}$. We have

$$\nabla G(\mathbf{Q}) = 2\mathbf{Q}^* \mathbf{\Lambda} \mathbf{Q}^{*T} \mathbf{Q} \mathbf{W}, \quad \nabla^2 G(\mathbf{Q})[\mathbf{D}] = 2\mathbf{Q}^* \mathbf{\Lambda} \mathbf{Q}^{*T} \mathbf{D} \mathbf{W}.$$

Therefore, by the formula for the Riemannian Hessian on the Stiefel manifold,

$$\begin{aligned} \text{Hess } G(\mathbf{Q}^*)[\mathbf{D}] &= \text{Proj}_{\mathbb{T}(\mathbf{Q}^*)} (\nabla^2 G(\mathbf{Q}^*)[\mathbf{D}] - \mathbf{D} \text{sym}(\mathbf{Q}^{*T} \nabla G(\mathbf{Q}^*))) \\ &= 2 \left(\mathbf{Q}^* \mathbf{\Lambda} \widehat{\mathbf{D}} \mathbf{W} - \mathbf{D} \mathbf{\Lambda} \mathbf{W} \right) - 2\mathbf{Q}^* \text{sym} \left(\mathbf{\Lambda} \widehat{\mathbf{D}} \mathbf{W} - \widehat{\mathbf{D}} \mathbf{\Lambda} \mathbf{W} \right). \end{aligned}$$

For any matrix \mathbf{M} , we have $\langle \mathbf{D}, \mathbf{Q}^* \text{sym}(\mathbf{M}) \rangle = \langle \widehat{\mathbf{D}}, \text{sym}(\mathbf{M}) \rangle = 0$, where the second equality follows from the fact that the inner product of a symmetric matrix and a skew-symmetric matrix is zero. Hence,

$$\langle \mathbf{D}, \text{Hess } G(\mathbf{Q}^*)[\mathbf{D}] \rangle = 2\text{Tr} \left(\widehat{\mathbf{D}}^T \mathbf{\Lambda} \widehat{\mathbf{D}} \mathbf{W} - (\mathbf{D}_1^T \mathbf{D}_1 + \widehat{\mathbf{D}}^T \widehat{\mathbf{D}}) \mathbf{\Lambda} \mathbf{W} \right). \quad (35)$$

Since $\lambda_1 > \dots > \lambda_K$ and $w_1 > \dots > w_K$, we first have

$$-\text{Tr}(\mathbf{D}_1^T \mathbf{D}_1 \mathbf{\Lambda} \mathbf{W}) \leq -\lambda_K w_K \|\mathbf{D}_1\|_F^2. \quad (36)$$

Writing $\widehat{\mathbf{D}} = (\widehat{d}_{ij})_{i,j=1}^K$, and using the skew-symmetry of $\widehat{\mathbf{D}}$, we compute

$$\begin{aligned} \text{Tr} \left(\widehat{\mathbf{D}}^T \mathbf{\Lambda} \widehat{\mathbf{D}} \mathbf{W} - \widehat{\mathbf{D}}^T \widehat{\mathbf{D}} \mathbf{\Lambda} \mathbf{W} \right) &= \sum_{i,j} \left(\lambda_j w_i \widehat{d}_{ji}^2 - \lambda_i w_i \widehat{d}_{ji}^2 \right) \\ &= -\frac{1}{2} \sum_{i,j} (w_j - w_i) (\lambda_j - \lambda_i) \widehat{d}_{ji}^2 \leq 0. \end{aligned} \quad (37)$$

Set

$$\delta_{\text{rot}} := \begin{cases} \left(\min_{i \in [K-1]} (w_i - w_{i+1}) \right) \left(\min_{i \in [K-1]} (\lambda_i - \lambda_{i+1}) \right), & K \geq 2, \\ +\infty, & K = 1. \end{cases}$$

For $K = 1$, we have $\widehat{\mathbf{D}} = \mathbf{0}$. Plugging (36) and (37) into (35) yields

$$\begin{aligned} \langle \mathbf{D}, \text{Hess } G(\mathbf{Q}^*)[\mathbf{D}] \rangle &\leq - \sum_{i,j} (w_j - w_i) (\lambda_j - \lambda_i) \widehat{d}_{ji}^2 - 2\lambda_K w_K \|\mathbf{D}_1\|_F^2 \\ &\leq - \min \{ \delta_{\text{rot}}, 2\lambda_K w_K \} \|\mathbf{D}\|_F^2, \end{aligned}$$

where we used the skew-symmetry of $\widehat{\mathbf{D}}$, the fact that its diagonal entries are zero, and $\|\mathbf{D}\|_F^2 = \|\widehat{\mathbf{D}}\|_F^2 + \|\mathbf{D}_1\|_F^2$. This proves (33) with $\delta_1 = \min \{ \delta_{\text{rot}}, 2\lambda_K w_K \}$.

(ii) If $\mathcal{Q}_G \setminus \mathcal{Q}_{\text{opt}} = \emptyset$, the claim is vacuous and we set $\delta_2 = 1$. Otherwise, define

$$\rho(\mathbf{Q}) := \max_{\mathbf{D} \in \text{T}(\mathbf{Q}), \|\mathbf{D}\|_F=1} \langle \mathbf{D}, \text{Hess } G(\mathbf{Q})[\mathbf{D}] \rangle.$$

The maximum is attained by compactness of the unit sphere in $\text{T}(\mathbf{Q})$. By Proposition 2, $\rho(\mathbf{Q}) > 0$ on $\mathcal{Q}_G \setminus \mathcal{Q}_{\text{opt}}$. This set is compact by Propositions 3 and 4 and Lemma 4, and ρ is continuous because the Riemannian Hessian depends continuously on \mathbf{Q} . Hence $\delta_2 := \frac{1}{2} \min_{\mathbf{Q} \in \mathcal{Q}_G \setminus \mathcal{Q}_{\text{opt}}} \rho(\mathbf{Q}) > 0$. For each $\mathbf{Q} \in \mathcal{Q}_G \setminus \mathcal{Q}_{\text{opt}}$, choosing a unit maximizer in the definition of $\rho(\mathbf{Q})$ gives (34). \square

4.3 Benign Optimization Landscape of HePPCA

In this subsection, we study the empirical problem of HePPCA, namely Problem (25). It is generally impossible to obtain a closed-form expression for the critical points of $F(\mathbf{Q})$. Fortunately, the critical points of its population counterpart $G(\mathbf{Q})$ can be fully characterized, as shown in Proposition 3. For ease of exposition, we denote the critical point set of F by

$$\mathcal{Q}_F := \{ \mathbf{Q} \in \text{St}(d, K) : \text{grad } F(\mathbf{Q}) = \mathbf{0} \}.$$

For each $k \in [K]$, define

$$\mathbf{\Delta}_k := \mathbf{A}_k - \mathbb{E}[\mathbf{A}_k]. \quad (38)$$

We first recall a global error bound obtained from [20, Corollary 1].

Lemma 5. *There exists a constant $\kappa_1 > 0$ such that, for all $\mathbf{Q} \in \text{St}(d, K)$,*

$$\text{dist}(\mathbf{Q}, \mathcal{Q}_G) \leq \kappa_1 \|\text{grad } G(\mathbf{Q})\|_F.$$

If $\mathcal{Q}_G \setminus \mathcal{Q}_{\text{opt}} = \emptyset$, we set $\text{dist}(\mathbf{Q}, \emptyset) = +\infty$ so the corresponding neighborhood assertions are vacuous. Lemma 5 controls the distance to \mathcal{Q}_G by the norm of Riemannian gradient of G . We next apply this bound to critical points of F , using the following perturbation identity. By (25), (27), and (28), for any $\mathbf{Q} \in \text{St}(d, K)$,

$$F(\mathbf{Q}) = G(\mathbf{Q}) + \sum_{k=1}^K \text{Tr}(\mathbf{Q}^T \Delta_k \mathbf{Q} \mathbf{E}_{kk}) + \sum_{k=1}^K \sum_{l=1}^L \frac{w_{l,k} n_l}{n}, \quad (39)$$

where $\mathbf{E}_{kk} := \mathbf{e}_k \mathbf{e}_k^T \in \mathbb{R}^{K \times K}$.

Lemma 6. *For each $\mathbf{Q} \in \mathcal{Q}_F$, we have*

$$\text{dist}(\mathbf{Q}, \mathcal{Q}_G) \leq 2\kappa_1 \sum_{k=1}^K \|\Delta_k\|, \quad (40)$$

where κ_1 is defined in Lemma 5.

Proof. For each $\mathbf{Q} \in \mathcal{Q}_F$, (39) gives

$$\mathbf{0} = \text{grad } F(\mathbf{Q}) = \text{grad } G(\mathbf{Q}) + \sum_{k=1}^K \text{grad } \text{Tr}(\mathbf{Q}^T \Delta_k \mathbf{Q} \mathbf{E}_{kk}).$$

Since Δ_k and \mathbf{E}_{kk} are symmetric, we have

$$\begin{aligned} \|\text{grad } G(\mathbf{Q})\|_F &= 2 \left\| \sum_{k=1}^K \text{Proj}_{\text{T}(\mathbf{Q})}(\Delta_k \mathbf{Q} \mathbf{E}_{kk}) \right\|_F \\ &\leq 2 \sum_{k=1}^K \|\Delta_k \mathbf{Q} \mathbf{E}_{kk}\|_F = 2 \sum_{k=1}^K \|\Delta_k \mathbf{q}_k\| \leq 2 \sum_{k=1}^K \|\Delta_k\|, \end{aligned}$$

where \mathbf{q}_k is the k -th column of \mathbf{Q} . Together with Lemma 5, this gives (40). \square

We next perturb the landscape of Problem (28) to analyze Problem (25) when \mathbf{A}_k is close to $\mathbb{E}[\mathbf{A}_k]$.

Proposition 6. *Suppose that $\{\Delta_k\}_{k=1}^K$ satisfy*

$$\sum_{k=1}^K \|\Delta_k\| \leq \frac{\min\{\delta_1, \delta_2\}}{12}, \quad (41)$$

where δ_1 and δ_2 are defined in Proposition 5. Then the following statements hold:

(i) *There exists $\gamma_1 > 0$ such that, for every $\mathbf{Q} \in \text{St}(d, K)$ satisfying*

$$\text{dist}(\mathbf{Q}, \mathcal{Q}_{\text{opt}}) \leq \gamma_1,$$

we have

$$\langle \mathbf{D}, \text{Hess } F(\mathbf{Q})[\mathbf{D}] \rangle \leq -\frac{\delta_1}{3} \|\mathbf{D}\|_F^2, \quad \forall \mathbf{D} \in \text{T}(\mathbf{Q}), \quad (42)$$

where \mathcal{Q}_{opt} is defined in Proposition 4.

(ii) There exists $\gamma_2 > 0$ such that, for every $\mathbf{Q} \in \text{St}(d, K)$ satisfying $\text{dist}(\mathbf{Q}, \mathcal{Q}_G \setminus \mathcal{Q}_{\text{opt}}) \leq \gamma_2$, there exists a nonzero $\mathbf{D} \in \mathbf{T}(\mathbf{Q})$ such that

$$\langle \mathbf{D}, \text{Hess } F(\mathbf{Q})[\mathbf{D}] \rangle \geq \frac{\delta_2}{3} \|\mathbf{D}\|_F^2. \quad (43)$$

Proof. From (39), we obtain

$$\text{Hess } F(\mathbf{Q}) = \text{Hess } G(\mathbf{Q}) + \sum_{k=1}^K \text{Hess } \text{Tr}(\mathbf{Q}^T \mathbf{\Delta}_k \mathbf{Q} \mathbf{E}_{kk}). \quad (44)$$

For each $\mathbf{D} \in \mathbf{T}(\mathbf{Q})$, we have

$$\begin{aligned} \nabla \text{Tr}(\mathbf{Q}^T \mathbf{\Delta}_k \mathbf{Q} \mathbf{E}_{kk}) &= 2\mathbf{\Delta}_k \mathbf{Q} \mathbf{E}_{kk}, \\ \nabla^2 \text{Tr}(\mathbf{Q}^T \mathbf{\Delta}_k \mathbf{Q} \mathbf{E}_{kk})[\mathbf{D}] &= \mathbf{\Delta}_k \mathbf{D} \mathbf{E}_{kk} + \mathbf{\Delta}_k^T \mathbf{D} \mathbf{E}_{kk}^T = 2\mathbf{\Delta}_k \mathbf{D} \mathbf{E}_{kk}, \end{aligned}$$

where $\mathbf{\Delta}_k$ and \mathbf{E}_{kk} are symmetric. By (2), nonexpansiveness of the tangent projection, $\|\mathbf{\Delta}_k \mathbf{D} \mathbf{E}_{kk}\|_F \leq \|\mathbf{\Delta}_k\| \|\mathbf{D}\|_F$ and $\|\text{sym}(\mathbf{Q}^T \mathbf{\Delta}_k \mathbf{Q} \mathbf{E}_{kk})\|_F \leq \|\mathbf{\Delta}_k\|$, we obtain

$$|\langle \mathbf{D}, \text{Hess } \text{Tr}(\mathbf{Q}^T \mathbf{\Delta}_k \mathbf{Q} \mathbf{E}_{kk})[\mathbf{D}] \rangle| \leq 4\|\mathbf{\Delta}_k\| \|\mathbf{D}\|_F^2.$$

This, together with (44), implies

$$|\text{Hess}(F-G)(\mathbf{Q})[\mathbf{D}, \mathbf{D}]| \leq 4\|\mathbf{D}\|_F^2 \sum_{k=1}^K \|\mathbf{\Delta}_k\|. \quad (45)$$

(i) It follows from Proposition 5(i), compactness of \mathcal{Q}_{opt} , and smoothness of G that there exists $\gamma_1 > 0$ such that for any $\tilde{\mathbf{Q}}$ in a neighborhood of \mathcal{Q}_{opt} , i.e.,

$$\tilde{\mathbf{Q}} \in \{\mathbf{Q} \in \text{St}(d, K) : \text{dist}(\mathbf{Q}, \mathcal{Q}_{\text{opt}}) \leq \gamma_1\},$$

the following inequality holds:

$$\langle \tilde{\mathbf{D}}, \text{Hess } G(\tilde{\mathbf{Q}})[\tilde{\mathbf{D}}] \rangle \leq -\frac{2}{3}\delta_1 \|\tilde{\mathbf{D}}\|_F^2, \quad \forall \tilde{\mathbf{D}} \in \mathbf{T}(\tilde{\mathbf{Q}}). \quad (46)$$

For each $\mathbf{Q} \in \text{St}(d, K)$ such that $\text{dist}(\mathbf{Q}, \mathcal{Q}_{\text{opt}}) \leq \gamma_1$, we have for all $\mathbf{D} \in \mathbf{T}(\mathbf{Q})$,

$$\langle \mathbf{D}, \text{Hess } F(\mathbf{Q})[\mathbf{D}] \rangle \leq 4 \sum_{k=1}^K \|\mathbf{\Delta}_k\| \cdot \|\mathbf{D}\|_F^2 + \langle \mathbf{D}, \text{Hess } G(\mathbf{Q})[\mathbf{D}] \rangle \leq -\frac{1}{3}\delta_1 \|\mathbf{D}\|_F^2,$$

where the first inequality follows from (45), and the last inequality uses (41) and (46).

(ii) If $\mathcal{Q}_G \setminus \mathcal{Q}_{\text{opt}} = \emptyset$, fix any $\gamma_2 > 0$. Otherwise, set $\mathcal{S} := \mathcal{Q}_G \setminus \mathcal{Q}_{\text{opt}}$. By Proposition 5(ii), for each $\mathbf{Q}_0 \in \mathcal{S}$, there is a unit direction $\mathbf{D}_0 \in \mathbf{T}(\mathbf{Q}_0)$ with $\langle \mathbf{D}_0, \text{Hess } G(\mathbf{Q}_0)[\mathbf{D}_0] \rangle \geq \delta_2$. For $\mathbf{Q} \in \text{St}(d, K)$, define $\mathbf{D}_{\mathbf{Q}_0}(\mathbf{Q}) := \text{Proj}_{\mathbf{T}(\mathbf{Q})}(\mathbf{D}_0)$. Since $\mathbf{D}_{\mathbf{Q}_0}(\mathbf{Q}_0) = \mathbf{D}_0 \neq \mathbf{0}$, from continuity of the tangent projection and the Riemannian Hessian, it follows that there exists $r_{\mathbf{Q}_0} > 0$ such

that $D_{\mathbf{Q}_0}(\mathbf{Q}) \neq \mathbf{0}$ and

$$\frac{\langle D_{\mathbf{Q}_0}(\mathbf{Q}), \text{Hess } G(\mathbf{Q})[D_{\mathbf{Q}_0}(\mathbf{Q})] \rangle}{\|D_{\mathbf{Q}_0}(\mathbf{Q})\|_F^2} \geq \frac{2\delta_2}{3}, \quad \forall \mathbf{Q} \in U_{\mathbf{Q}_0},$$

where $U_{\mathbf{Q}_0} := \{\mathbf{Q} \in \text{St}(d, K) : \|\mathbf{Q} - \mathbf{Q}_0\|_F < r_{\mathbf{Q}_0}\}$. The sets $\{U_{\mathbf{Q}_0} : \mathbf{Q}_0 \in \mathcal{S}\}$ form an open cover of compact \mathcal{S} , so there exist $\mathbf{Q}_1, \dots, \mathbf{Q}_m \in \mathcal{S}$ such that $\mathcal{S} \subseteq \bigcup_{i=1}^m U_{\mathbf{Q}_i}$. Set $U := \bigcup_{i=1}^m U_{\mathbf{Q}_i}$. Since U is an open neighborhood of compact \mathcal{S} in $\text{St}(d, K)$, choose $\gamma_2 > 0$ such that

$$\{\mathbf{Q} \in \text{St}(d, K) : \text{dist}(\mathbf{Q}, \mathcal{S}) \leq \gamma_2\} \subseteq U.$$

Thus, if $\text{dist}(\mathbf{Q}, \mathcal{S}) \leq \gamma_2$, then $\mathbf{Q} \in U_{\mathbf{Q}_i}$ for some i . Taking $\mathbf{D} := D_{\mathbf{Q}_i}(\mathbf{Q}) = \text{Proj}_{\mathbb{T}(\mathbf{Q})}(\mathbf{D}_0^i)$, where $\mathbf{D}_0^i \in \mathbb{T}(\mathbf{Q}_i)$ is the corresponding unit direction, gives $\mathbf{D} \neq \mathbf{0}$ and $\langle \mathbf{D}, \text{Hess } G(\mathbf{Q})[\mathbf{D}] \rangle \geq (2\delta_2/3)\|\mathbf{D}\|_F^2$. Combining this with (41) and (45) gives (43). \square

To proceed, we introduce the following definitions. Let $\mathcal{B}_{\text{geo}}(\mathbf{Q}_0, \eta)$ denote a geodesic ball in $\text{St}(d, K)$ centered at \mathbf{Q}_0 with radius η with respect to the Riemannian metric. A subset $S \subseteq \text{St}(d, K)$ is called geodesically convex if any two points in S can be joined by a geodesic segment lying entirely in S (see [3, Chapter 11]).

Lemma 7. *Let $H : \text{St}(d, K) \rightarrow \mathbb{R}$ be a smooth function. Let $\eta > 0$ be such that the geodesic ball $\mathcal{B}_{\text{geo}}(\mathbf{Q}_0, \eta)$ is geodesically convex. Suppose that there exists $\mu > 0$ such that*

$$\langle \mathbf{D}, \text{Hess } H(\mathbf{Z})[\mathbf{D}] \rangle \leq -\mu\|\mathbf{D}\|_F^2, \quad \forall \mathbf{Z} \in \mathcal{B}_{\text{geo}}(\mathbf{Q}_0, \eta), \mathbf{D} \in \mathbb{T}(\mathbf{Z}).$$

Then $\mathcal{B}_{\text{geo}}(\mathbf{Q}_0, \eta)$ contains at most one critical point of H .

Proof. Suppose that two distinct critical points $\mathbf{Q}_a, \mathbf{Q}_b$ of H lie in $\mathcal{B}_{\text{geo}}(\mathbf{Q}_0, \eta)$. By geodesic convexity, they are connected by a nonconstant geodesic γ contained in this ball. For $\varphi := H \circ \gamma$, the Hessian bound gives

$$\varphi''(t) = \langle \dot{\gamma}(t), \text{Hess } H(\gamma(t))[\dot{\gamma}(t)] \rangle \leq -\mu\|\dot{\gamma}(t)\|_F^2 < 0.$$

Hence φ' is strictly decreasing. On the other hand, since \mathbf{Q}_a and \mathbf{Q}_b are critical points of H , we have $\varphi'(0) = \varphi'(1) = 0$, a contradiction. \square

We next fix several constants used later. Since \mathcal{Q}_{opt} is finite, by the local geodesic convexity of sufficiently small geodesic balls, Proposition 5(i), and the continuity of the Riemannian Hessian of G , we can choose $\eta > 0$ such that, for every $\mathbf{Q}_1 \in \mathcal{Q}_{\text{opt}}$, the geodesic ball $\mathcal{B}_{\text{geo}}(\mathbf{Q}_1, \eta)$ is geodesically convex, is contained in the γ_1 -neighborhood of \mathcal{Q}_{opt} , and satisfies

$$\text{Hess } G(\mathbf{Z})[\mathbf{D}, \mathbf{D}] \leq -\frac{\delta_1}{2}\|\mathbf{D}\|_F^2, \quad \forall \mathbf{Z} \in \mathcal{B}_{\text{geo}}(\mathbf{Q}_1, \eta), \mathbf{D} \in \mathbb{T}(\mathbf{Z}).$$

Moreover, since each $\mathcal{B}_{\text{geo}}(\mathbf{Q}_1, \eta)$ is an open neighborhood of \mathbf{Q}_1 in $\text{St}(d, K)$ and \mathcal{Q}_{opt} is finite, there exists $\tau > 0$ such that

$$\mathbb{B}(\mathbf{Q}_1, \tau) \cap \text{St}(d, K) \subseteq \mathcal{B}_{\text{geo}}(\mathbf{Q}_1, \eta), \quad \forall \mathbf{Q}_1 \in \mathcal{Q}_{\text{opt}},$$

where $\mathbb{B}(\mathbf{Q}_1, \tau) := \{\mathbf{Q} : \|\mathbf{Q} - \mathbf{Q}_1\|_F \leq \tau\}$.

Set

$$\sigma_0 := \begin{cases} \text{dist}(\mathcal{Q}_{\text{opt}}, \mathcal{Q}_G \setminus \mathcal{Q}_{\text{opt}}), & \mathcal{Q}_G \setminus \mathcal{Q}_{\text{opt}} \neq \emptyset, \\ 1, & \mathcal{Q}_G \setminus \mathcal{Q}_{\text{opt}} = \emptyset, \end{cases} \quad c_0 := 1/2.$$

Then, we prove that $\sigma_0 > 0$. If $\mathcal{Q}_G \setminus \mathcal{Q}_{\text{opt}} = \emptyset$, this follows directly from the definition. Otherwise, fix any $\mathbf{Q}_1 \in \mathcal{Q}_{\text{opt}}$. By the choice of η , the ball $\mathcal{B}_{\text{geo}}(\mathbf{Q}_1, \eta)$ is geodesically convex and $\text{Hess}G$ is negative definite on this ball. Applying Lemma 7 with $H = G$, we conclude that each $\mathbf{Q}_1 \in \mathcal{Q}_{\text{opt}}$ is isolated in \mathcal{Q}_G . Since \mathcal{Q}_{opt} is finite and \mathcal{Q}_G is compact, it follows that $\sigma_0 > 0$. We now state the perturbation result for Problem (25).

Theorem 3. *Suppose that $\{\Delta_k\}_{k=1}^K$ satisfies*

$$\sum_{k=1}^K \|\Delta_k\| \leq \delta_3 := \min \left\{ \frac{\min\{\gamma_1, \gamma_2, \tau, \sigma_0/3, c_0\}}{2\kappa_1}, \frac{\min\{\delta_1, \delta_2\}}{12} \right\}, \quad (47)$$

where γ_1, γ_2 are defined in Proposition 6, δ_1, δ_2 are defined in Proposition 5, τ, σ_0, c_0 are fixed above, and κ_1 is defined in Lemma 5. Then every $\mathbf{Q} \in \mathcal{Q}_F$ is either a global maximizer or a strict saddle point. In particular, if \mathbf{Q} is a global maximizer, then F is locally geodesically strongly concave near \mathbf{Q} .

Proof. Obviously, it follows from (47) that (41) holds. This, together with Proposition 6, yields that (42) and (43) hold. Moreover, using Lemma 6 and (47), we have $\text{dist}(\mathbf{Q}, \mathcal{Q}_G) \leq \min\{\gamma_1, \gamma_2, c_0, \tau, \sigma_0/3\}$ for any $\mathbf{Q} \in \mathcal{Q}_F$. For simplicity, let $r := \min\{\gamma_1, \gamma_2, c_0, \tau, \sigma_0/3\}$. Thus every $\mathbf{Q} \in \mathcal{Q}_F$ is r -close to \mathcal{Q}_{opt} or to $\mathcal{Q}_G \setminus \mathcal{Q}_{\text{opt}}$. The choice $r \leq \sigma_0/3$ separates the two population critical sets when both are nonempty.

Case 1. Suppose that $\mathbf{Q} \in \mathcal{Q}_F$ satisfies $\text{dist}(\mathbf{Q}, \mathcal{Q}_G \setminus \mathcal{Q}_{\text{opt}}) \leq r$. This, together with (43), implies that \mathbf{Q} is a strict saddle point, and thus not a global maximizer.

Case 2. Suppose that $\mathbf{Q} \in \mathcal{Q}_F$ satisfies $\text{dist}(\mathbf{Q}, \mathcal{Q}_{\text{opt}}) \leq r$. Since \mathcal{Q}_{opt} consists of finitely many isolated points as defined in (32), whose pairwise distances are at least 2 due to $\mathbf{s}, \mathbf{t} \in \{1, -1\}^K$, and $r \leq c_0 = 1/2 < 1$, there exists a unique $\mathbf{Q}_\star \in \mathcal{Q}_{\text{opt}}$ such that

$$\|\mathbf{Q}_\star - \mathbf{Q}\|_F = \min \{\|\mathbf{U} - \mathbf{Q}\|_F : \mathbf{U} \in \mathcal{Q}_{\text{opt}}\}.$$

By $r \leq \tau$, we have $\mathbf{Q} \in \mathcal{B}_{\text{geo}}(\mathbf{Q}_\star, \eta)$. Since (42) holds throughout $\mathcal{B}_{\text{geo}}(\mathbf{Q}_\star, \eta)$, Lemma 7 shows that \mathbf{Q} is the unique critical point of F in this neighborhood.

It remains to show that \mathbf{Q} is a global maximizer. Suppose, for contradiction, that it is not. Since $\text{St}(d, K)$ is compact and F is continuous, there exists a global maximizer $\widehat{\mathbf{Q}}$. Then $\widehat{\mathbf{Q}} \in \mathcal{Q}_F$ and $F(\widehat{\mathbf{Q}}) > F(\mathbf{Q})$. The point $\widehat{\mathbf{Q}}$ cannot fall under **Case 1**, since every point in **Case 1** is a strict saddle point. Therefore, $\text{dist}(\widehat{\mathbf{Q}}, \mathcal{Q}_{\text{opt}}) \leq r$. Using the same argument as above, there exists a unique $\widehat{\mathbf{Q}}_\star \in \mathcal{Q}_{\text{opt}}$ such that

$$\|\widehat{\mathbf{Q}}_\star - \widehat{\mathbf{Q}}\|_F = \min \{\|\mathbf{U} - \widehat{\mathbf{Q}}\|_F : \mathbf{U} \in \mathcal{Q}_{\text{opt}}\}.$$

By Proposition 4, there exists $\mathbf{s} \in \{1, -1\}^K$ such that $\mathbf{Q}_\star = \widehat{\mathbf{Q}}_\star \text{diag}(\mathbf{s})$. Moreover, by the

definition of F in (25) and (26), we have

$$F(\mathbf{Z}) = F(\mathbf{Z}\text{diag}(\mathbf{s})), \quad \forall \mathbf{Z} \in \text{St}(d, K). \quad (48)$$

Thus, we obtain $F(\widehat{\mathbf{Q}}) = F(\widehat{\mathbf{Q}}\text{diag}(\mathbf{s}))$. Also, by $\mathbf{s} \in \{1, -1\}^K$, we have $\|\mathbf{Q}_* - \widehat{\mathbf{Q}}\text{diag}(\mathbf{s})\|_F = \|\widehat{\mathbf{Q}}_* - \widehat{\mathbf{Q}}\|_F \leq r$. Therefore, $\widehat{\mathbf{Q}}\text{diag}(\mathbf{s})$ is also a global maximizer by (48) and $\widehat{\mathbf{Q}}\text{diag}(\mathbf{s}) \in \mathcal{B}_{\text{geo}}(\mathbf{Q}_*, \eta)$ because $r \leq \tau$. Moreover, $\widehat{\mathbf{Q}}\text{diag}(\mathbf{s}) \neq \mathbf{Q}$; otherwise, (48) would imply $F(\widehat{\mathbf{Q}}) = F(\mathbf{Q})$, contradicting $F(\widehat{\mathbf{Q}}) > F(\mathbf{Q})$. Thus, $\mathcal{B}_{\text{geo}}(\mathbf{Q}_*, \eta)$ contains two distinct critical points, namely \mathbf{Q} and $\widehat{\mathbf{Q}}\text{diag}(\mathbf{s})$, contradicting the uniqueness established above. Hence, \mathbf{Q} must be a global maximizer.

Finally, let \mathbf{Q} be any global maximizer of F . **By Case 2**, \mathbf{Q} lies near some $\mathbf{Q}_* \in \mathcal{Q}_{\text{opt}}$; applying (42) on a smaller neighborhood gives local geodesic strong concavity. This completes the proof. \square

It is worth noting that [9, Lemma F.14] and [25, Lemma 3] have established concentration bounds for the deviation of the sample covariance matrix of Gaussian random vectors from its expectation as follows. Recall that $\mathbf{y}_{l,i} \sim \mathcal{N}(\mathbf{0}, \mathbf{Q}^* \boldsymbol{\Lambda} \mathbf{Q}^{*T} + v_l \mathbf{I}_d)$, as defined in (24) and let

$$\mathbf{C}_l := \frac{1}{n} \sum_{i=1}^{n_l} \mathbf{y}_{l,i} \mathbf{y}_{l,i}^T, \quad \xi_l := \frac{\sum_{k=1}^K \lambda_k + v_l d}{\lambda_1 + v_l}. \quad (49)$$

Lemma 8. *For each fixed $l \in [L]$ and each $t > 0$, it holds with probability at least $1 - e^{-t}$ that*

$$\|\mathbf{C}_l - \mathbb{E}[\mathbf{C}_l]\| \leq \frac{c_1 n_l}{n} (\lambda_1 + v_l) \max \left\{ \sqrt{\frac{\xi_l \log d + t}{n_l}}, \frac{\xi_l \log d + t}{n_l} \log n \right\},$$

where $c_1 > 0$ is a universal constant.

By setting $t = \log n$ in the above lemma and applying the union bound, we obtain the following corollary.

Corollary 1. *It holds with probability at least $1 - L/n$ that for all $l \in [L]$,*

$$\|\mathbf{C}_l - \mathbb{E}[\mathbf{C}_l]\| \leq \frac{c_1 n_l (\lambda_1 + v_l)}{n} \max \left\{ \sqrt{\frac{\xi_l \log d + \log n}{n_l}}, \frac{\xi_l \log d + \log n}{n_l} \log n \right\}, \quad (50)$$

where $c_1 > 0$ is a universal constant.

Before proceeding, we note that for every $l \in [L]$,

$$\xi_l = \frac{\sum_{k=1}^K \lambda_k + v_l d}{\lambda_1 + v_l} \leq \frac{d \lambda_1 + v_l d}{\lambda_1 + v_l} = d, \quad (51)$$

where the inequality follows from $\sum_{k=1}^K \lambda_k \leq K \lambda_1 \leq d \lambda_1$. Using Theorem 3 and Corollary 1, we are ready to show the optimization landscape of the HePPCA problem (25) when the number of training samples satisfies a suitable lower bound.

Theorem 4. Let $n_{\min} := \min_l n_l$ and $v_{\min} := \min_l v_l$. Suppose that

$$n_{\min} \geq \max \left\{ \log^2 n, \left(\frac{c_1 \lambda_1 K}{v_{\min} \delta_3} \right)^2 \right\} (d \log d + \log n), \quad (52)$$

where δ_3 is defined in Theorem 3 and c_1 in Corollary 1. Then, with probability at least $1 - L/n$, every $\mathbf{Q} \in \mathcal{Q}_F$ is either a global maximizer or a strict saddle point. In particular, if \mathbf{Q} is a global maximizer, then F is locally geodesically strongly concave near \mathbf{Q} .

Proof. Suppose that (50) holds for each $l \in [L]$, which happens with probability at least $1 - L/n$. According to (38) and (49), we have

$$\|\Delta_k\| = \left\| \sum_{l \in [L]} \frac{w_{l,k}}{v_l} (\mathbf{C}_l - \mathbb{E}[\mathbf{C}_l]) \right\|.$$

This implies

$$\begin{aligned} \sum_{k=1}^K \|\Delta_k\| &\leq \sum_{k=1}^K \sum_{l=1}^L \frac{w_{l,k}}{v_l} \|\mathbf{C}_l - \mathbb{E}[\mathbf{C}_l]\| \\ &\leq \frac{c_1}{n} \sum_{k=1}^K \sum_{l=1}^L \frac{w_{l,k} n_l}{v_l} (\lambda_1 + v_l) \max \left\{ \sqrt{\frac{\xi_l \log d + \log n}{n_l}}, \frac{\xi_l \log d + \log n}{n_l} \log n \right\} \\ &\leq \frac{c_1 \lambda_1 K}{n} \sum_{l=1}^L \frac{n_l}{v_l} \max \left\{ \sqrt{\frac{d \log d + \log n}{n_l}}, \frac{d \log d + \log n}{n_l} \log n \right\}, \end{aligned}$$

where the second inequality uses (50), the third inequality follows from $w_{l,k} \leq \lambda_1 / (\lambda_1 + v_l)$ by (26) and (51). Using the above inequality and $n_l \geq n_{\min} \geq (d \log d + \log n) \log^2 n$ from (52) yields

$$\sum_{k=1}^K \|\Delta_k\| \leq \frac{c_1 \lambda_1 K}{n} \sum_{l=1}^L \frac{n_l}{v_l} \sqrt{\frac{d \log d + \log n}{n_l}} \leq \frac{c_1 \lambda_1 K}{v_{\min}} \sqrt{\frac{d \log d + \log n}{n_{\min}}}.$$

This, together with (52), implies $\sum_{k=1}^K \|\Delta_k\| \leq \delta_3$. It follows from this and Theorem 3 that the desired result holds. \square

5 Experimental Results

In this section, we conduct numerical experiments on the QPOC and HePPCA problems to illustrate the convergence behavior predicted by our theoretical results.

5.1 Benign optimization landscape of QPOC Problems

In this subsection, we conduct numerical experiments on synthetic data to validate the theoretical results in Theorem 2. To this end, we apply Riemannian gradient ascent (RGA) to solve Problem (1) and examine whether it converges to a global maximizer from different random initializations. For each random initialization, we generate a Gaussian random matrix $\mathbf{Z} \in \mathbb{R}^{d \times K}$

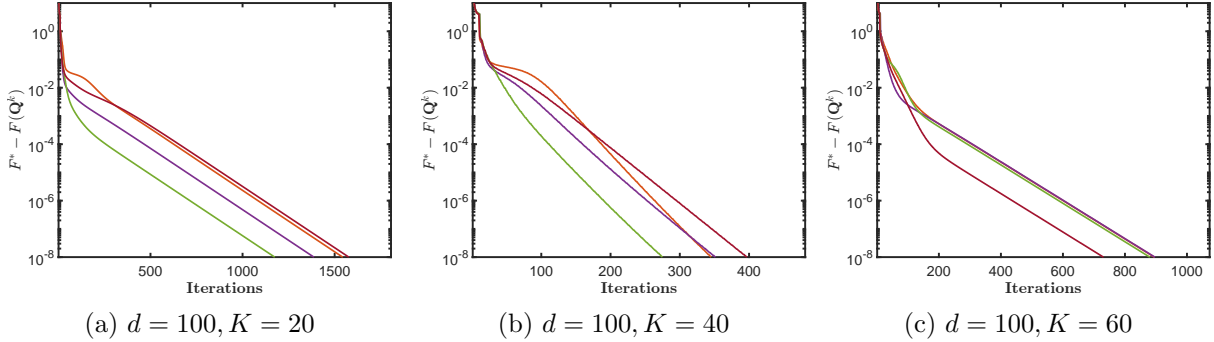


Figure 2: **Convergence performance of Riemannian GA for solving QPOC.** The x -axis is number of iterations k , and y -axis is the function value gap $F^* - F^k$. Here, $F^k := F(\mathbf{Q}^k)$ denotes the function value at the k -th iterate \mathbf{Q}^k generated by Riemannian GA, and F^* is the optimal value of Problem (1).

and compute its compact SVD $\mathbf{Z} = \mathbf{U}\mathbf{\Sigma}\mathbf{V}^T$, where $\mathbf{U} \in \text{St}(d, K)$ and $\mathbf{V} \in \mathcal{O}^K$. We then set $\mathbf{Q}^0 = \mathbf{U}\mathbf{V}^T$.

In our experiments, we set $d = 100$ and $K \in \{20, 40, 60\}$, and generate the matrices $\mathbf{A} \in \mathbb{S}^d$ and $\mathbf{B} \in \mathbb{S}^K$ as follows. Specifically, we generate a vector $\mathbf{a} \in \mathbb{R}^d$ by sampling its entries independently from the uniform distribution on $[5, 10]$ and then sorting them in descending order. Similarly, we generate a vector $\mathbf{b} \in \mathbb{R}^K$ by sampling the first $K/2$ entries from the uniform distribution on $[1, 1.1]$ and the remaining entries from the uniform distribution on $[-1, -0.9]$, after which the entries are sorted in descending order. We then set $\mathbf{A} = \text{diag}(\mathbf{a})$ and $\mathbf{B} = \text{diag}(\mathbf{b})$.

Based on the above setup, we run RGA from four different random initializations and visualize the convergence behavior in terms of the optimality gap $F^* - F^k$ for solving Problem (1); see Figure 2. Here, $F^k := F(\mathbf{Q}^k)$ denotes the function value at the k -th iterate \mathbf{Q}^k generated by RGA, and F^* is the optimal value of Problem (1), computed according to (20). It can be observed that, regardless of the random initialization, RGA consistently converges to a global maximizer at a linear rate. This behavior empirically supports the theoretical results in Theorem 2 regarding the benign optimization landscape of Problem (1).

5.2 Experiments on HePPCA

In this subsection, we conduct numerical experiments on synthetic data to validate the theoretical results in Theorem 4. First, we generate the samples $\{\mathbf{y}_{l,i}\}$ according to the HePPCA model (24). Specifically, we set the total dimension $d = 20$, the subspace dimension $K = 3$, the number of groups $L = 2$, $\boldsymbol{\lambda} = (3, 2, 0.5)$ and $\mathbf{v} = (0.2, 0.1)$. The ground-truth subspace matrix $\mathbf{Q}^* \in \text{St}(d, K)$ is generated by first sampling a Gaussian random matrix $\mathbf{G} \in \mathbb{R}^{d \times K}$ with i.i.d. standard normal entries and then computing its QR decomposition $\mathbf{G} = \mathbf{Q}\mathbf{R}$, where $\mathbf{Q} \in \text{St}(d, K)$ and $\mathbf{R} \in \mathbb{R}^{K \times K}$ is upper triangular. Then, we set $\mathbf{Q}^* = \mathbf{Q}$, which has orthonormal columns. Next, we generate three independent sets of samples $\{\mathbf{y}_{l,i}\}$ and construct the corresponding data matrices $\{\mathbf{A}_k\}_{k=1}^K$ according to (26).

Based on the above setup, we run RGA from four different random initializations, as described in Section 5.1, and stop the algorithm when the Riemannian gradient norm is smaller

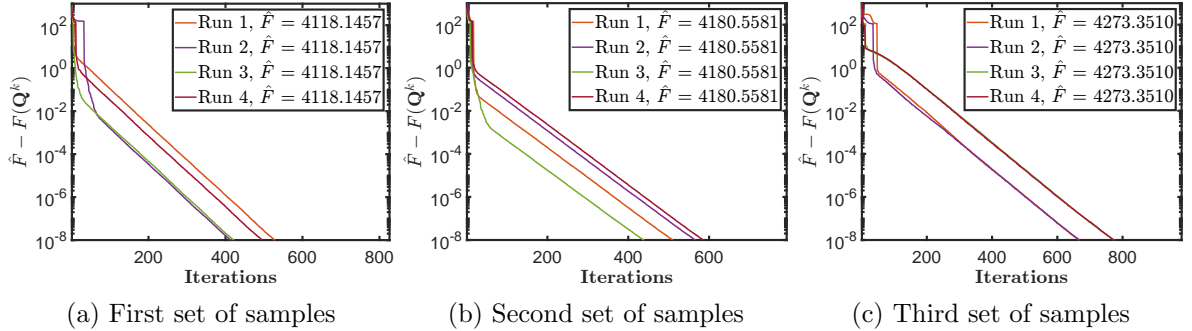


Figure 3: **Convergence performance of Riemannian GA for solving HePPCA.** The x -axis is number of iterations k , and y -axis is the function value gap $\hat{F} - F^k$. Here, $F^k = F(\mathbf{Q}^k)$ denotes the function value at the k -th iterate \mathbf{Q}^k , and \hat{F} denotes the function value at the final iterate.

than 10^{-6} . We first visualize the convergence performance of Riemannian GA for solving Problem (25) in terms of $\hat{F} - F^k$ in Figure 3, where $F^k = F(\mathbf{Q}^k)$ denotes the function value at the k -th iterate \mathbf{Q}^k , and \hat{F} denotes the function value at the final iterate. It can be observed that RGA appears to converge to an optimal solution, reaching the same function value across different runs with a linear rate. This behavior empirically supports the theoretical results in Theorem 4 regarding the benign optimization landscape of Problem (25).

6 Conclusion

In this work, we establish a complete characterization of the optimization landscape of QPOC by showing that every critical point is either a global maximizer or a strict saddle point. As an application, we show that the population objective of HePPCA is a special instance of QPOC and enjoys both a benign landscape and local geodesic strong concavity near every global maximizer. We further prove that, under a sufficiently large groupwise sample-size condition, the finite-sample HePPCA objective inherits these properties with high probability, thereby supporting the observed local linear convergence of retraction-based methods. A natural future direction is to extend the benign landscape analysis to other manifold optimization problems arising in modern machine learning, such as maximal coding rate reduction [5] and neural collapse [32]. Another interesting direction is to investigate nonhomogeneous QPOC problems that include an additional linear term in the objective.

References

- [1] E. M. Achour, F. Malgouyres, and S. Gerchinovitz. The loss landscape of deep linear neural networks: A second-order analysis. *Journal of Machine Learning Research*, 25(242):1–76, 2024.
- [2] S. Bhojanapalli, B. Neyshabur, and N. Srebro. Global optimality of local search for low rank matrix recovery. In *Advances in Neural Information Processing Systems*, volume 29, 2016.

- [3] N. Boumal. *An Introduction to Optimization on Smooth Manifolds*. Cambridge University Press, 2023.
- [4] J. S. Cavazos, J. A. Fessler, and L. Balzano. ALPCAH: Sample-wise heteroscedastic pca with tail singular value regularization. In *International Conference on Sampling Theory and Applications*, pages 1–6. IEEE, 2023.
- [5] K. H. R. Chan, Y. Yu, C. You, H. Qi, J. Wright, and Y. Ma. Redunet: A white-box deep network from the principle of maximizing rate reduction. *Journal of Machine Learning Research*, 23(114):1–103, 2022.
- [6] P. Chen, R. Jiang, and P. Wang. A complete loss landscape analysis of regularized deep matrix factorization. *arXiv preprint arXiv:2506.20344*, 2025.
- [7] Y. Chi, Y. M. Lu, and Y. Chen. Nonconvex optimization meets low-rank matrix factorization: An overview. *IEEE Transactions on Signal Processing*, 67(20):5239–5269, 2019.
- [8] R. Ge, C. Jin, and Y. Zheng. No spurious local minima in nonconvex low rank problems: A unified geometric analysis. In *International Conference on Machine Learning*, pages 1233–1242. PMLR, 2017.
- [9] K. Gilman, S. Burer, and L. Balzano. A semidefinite relaxation for sums of heterogeneous quadratic forms on the Stiefel manifold. *SIAM Journal on Matrix Analysis and Applications*, 46(2):1091–1116, 2025.
- [10] K. Gilman, D. Hong, J. A. Fessler, and L. Balzano. Streaming heteroscedastic probabilistic PCA with missing data. *Transactions on Machine Learning Research*, 2025. ISSN 2835-8856.
- [11] W. Givens. Computation of plain unitary rotations transforming a general matrix to triangular form. *Journal of the Society for Industrial and Applied Mathematics*, 6(1):26–50, 1958.
- [12] G. H. Golub and C. F. Van Loan. *Matrix Computations*. JHU press, 2013.
- [13] D. Hong, K. Gilman, L. Balzano, and J. A. Fessler. HePPCAT: Probabilistic PCA for data with heteroscedastic noise. *IEEE Transactions on Signal Processing*, 69:4819–4834, 2021.
- [14] R. A. Horn and C. R. Johnson. *Matrix analysis*. Cambridge University Press, 2012.
- [15] E. L. Lawler. The quadratic assignment problem. *Management Science*, 9(4):586–599, 1963.
- [16] J. D. Lee, I. Panageas, G. Piliouras, M. Simchowitz, M. I. Jordan, and B. Recht. First-order methods almost always avoid strict saddle points. *Mathematical Programming*, 176(1):311–337, 2019.
- [17] X. Li, J. Lu, R. Arora, J. Haupt, H. Liu, Z. Wang, and T. Zhao. Symmetry, saddle points, and global optimization landscape of nonconvex matrix factorization. *IEEE Transactions on Information Theory*, 65(6):3489–3514, 2019.

- [18] S. Ling. Solving orthogonal group synchronization via convex and low-rank optimization: Tightness and landscape analysis. *Mathematical Programming*, 200(1):589–628, 2023.
- [19] S. Ling. Local geometry determines global landscape in low-rank factorization for synchronization. *Foundations of Computational Mathematics*, 26:1553–1585, 2026.
- [20] H. Liu, A. M.-C. So, and W. Wu. Quadratic optimization with orthogonality constraint: explicit Lojasiewicz exponent and linear convergence of retraction-based line-search and stochastic variance-reduced gradient methods. *Mathematical Programming*, 178(1):215–262, 2019.
- [21] A. D. McRae and N. Boumal. Benign landscapes of low-dimensional relaxations for orthogonal synchronization on general graphs. *SIAM Journal on Optimization*, 34(2):1427–1454, 2024.
- [22] A. D. McRae, P. Abdalla, A. S. Bandeira, and N. Boumal. Nonconvex landscapes for Z_2 synchronization and graph clustering are benign near exact recovery thresholds. *Information and Inference: A Journal of the IMA*, 14(2):iaaf012, 2025.
- [23] S. T. Smith. Optimization techniques on Riemannian manifolds. *arXiv preprint arXiv:1407.5965*, 2014.
- [24] J. Sun, Q. Qu, and J. Wright. A geometric analysis of phase retrieval. *Foundations of Computational Mathematics*, 18(5):1131–1198, 2018.
- [25] J. Wang, C. Jiang, H. Liu, and A. M.-C. So. On the estimation performance of the generalized power method for heteroscedastic probabilistic PCA. *arXiv preprint arXiv:2312.03438*, 2023.
- [26] P. Wang, H. Liu, D. Pai, Y. Yu, Z. Zhu, Q. Qu, and Y. Ma. A global geometric analysis of maximal coding rate reduction. In *International Conference on Machine Learning*, volume 235, pages 51012–51040. PMLR, 2024.
- [27] Z. Wen and W. Yin. A feasible method for optimization with orthogonality constraints. *Mathematical Programming*, 142(1):397–434, 2013.
- [28] N. Xiao and X. Liu. Solving optimization problems over the stiefel manifold by smooth exact penalty function. *arXiv preprint arXiv:2110.08986*, 2021.
- [29] N. Xiao, X. Liu, and Y.-x. Yuan. A class of smooth exact penalty function methods for optimization problems with orthogonality constraints. *Optimization Methods and Software*, 37(4):1205–1241, 2022.
- [30] A. S. Xu, L. Balzano, and J. A. Fessler. HeMPPCAT: mixtures of probabilistic principal component analysers for data with heteroscedastic noise. In *IEEE International Conference on Acoustics, Speech and Signal Processing*, pages 1–5. IEEE, 2023.
- [31] Y. Yan, Y. Chen, and J. Fan. Inference for heteroskedastic PCA with missing data. *The Annals of Statistics*, 52(2):729–756, 2024.

- [32] C. Yaras, P. Wang, Z. Zhu, L. Balzano, and Q. Qu. Neural collapse with normalized features: A geometric analysis over the Riemannian manifold. In *Advances in Neural Information Processing Systems*, volume 35, pages 11547–11560, 2022.
- [33] A. R. Zhang, T. T. Cai, and Y. Wu. Heteroskedastic PCA: Algorithm, optimality, and applications. *The Annals of Statistics*, 50(1):53–80, 2022.
- [34] Z. Zhu, T. Ding, J. Zhou, X. Li, C. You, J. Sulam, and Q. Qu. A geometric analysis of neural collapse with unconstrained features. In *Advances in Neural Information Processing Systems*, volume 34, pages 29820–29834, 2021.